Published in final edited form as:
J Cell Physiol. 2008 October ; 217(1): 113–126. doi:10.1002/jcp.21482.

Expression of Secreted Frizzled Related Protein 1, A Wnt Antagonist, in Brain, Kidney, and Skeleton is Dispensable for Normal Embryonic Development

Brune Trevant[1], **Tripti Gaur**[1], **Sadiq Hussain**[1], **John Symons**[1], **Barry S. Komm**[2], **Peter V.N. Bodine**[2], **Gary S. Stein**[1], and **Jane B. Lian**[1,*]

[1]Department of Cell Biology and Cancer Center, University of Massachusetts Medical School, Worcester, Massachusetts

[2]Women's Health and Musculoskeletal Biology, Wyeth Research, Collegeville, Pennsylvania

Abstract

Secreted frizzled related protein-1 (sFRP1), an antagonist of Wnt signaling, regulates cell proliferation, differentiation and apoptosis and negatively regulates bone formation. The spatial and temporal pattern of endogenous sFRP1 expression and loss-of-function were examined in the sFRP1-LacZ knock-in mouse (sFRP1$^{-/-}$) during embryonic development and post-natal growth. β-gal activity representing sFRP1 expression is robust in brain, skeleton, kidney, eye, spleen, abdomen, heart and somites in early embryos, but sFRP1 gene inactivation in these tissues did not compromise normal embryonic and post-natal development. Kidney histology revealed increased numbers of glomeruli in KO mice, observed after 5 years of breeding. In the skeleton, we show sFRP1 expression is found in relation to the mineralizing front of bone tissue during skeletal development from E15.5 to birth. Trabecular bone volume and bone mineral density in the sFRP1$^{-/-}$ mouse compared to WT was slightly increased during post-natal growth. Calvarial osteoblasts from newborn sFRP1$^{-/-}$ mice exhibited a 20% increase in cell proliferation and differentiation at the early stages of osteoblast maturation. sFRP1 expression was observed in osteoclasts, but this did not affect osteoclast number or activity. These findings have identified functions for sFRP1 in kidney and bone that are not redundant with other sFRPs. In summary, the absence of major organ abnormalities, the enhanced bone formation and a normal life span with no detection of spontaneous tumors suggests that targeting sFRP1 can be used as a therapeutic strategy for increasing bone mass in metabolic bone disorders or promoting fracture healing by modulating Wnt signaling.

The Wnt signaling pathway is involved in the regulation of embryonic development, induction of cell polarity, self renewal of hematopoietic stem cells, determination of cell fate and apoptosis (Eaves, 2003; Reya et al., 2003; Willert et al., 2003; Nusse, 2005). At least 19 different Wnt proteins, a family of secreted cysteine rich glycoprotein, are known whose function is transduced via several pathways following binding to the seven transmembrane

*Correspondence to: Jane B. Lian, Department of Cell Biology, University of Massachusetts Medical School, 55 Lake Avenue North, Worcester, MA 01655. jane.lian@umasssmed.edu.

domain receptors of the frizzled (FZD) family (Nusse, 2005). A canonical β-catenin pathway is activated in most tissues for its nuclear translocation to induce gene transcription as a coregulatory protein with the LEF (lymphocyte enhancer factor)/T-cell transcription factor (Behrens et al., 1996). Other Wnt downstream cascades include a planar cell polarity pathway which involves RhoA and JNK activation of AP-1 target genes to regulate cell shape and movement (Veeman et al., 2003) and the Wnt-calcium pathway which is implicated in cell migration and involves Wnt signaling via a G-protein coupled receptor complex (Wang and Malbon, 2003; Kuhl, 2004). Non-canonical pathways can even antagonize the canonical pathway (Kuhl et al., 2001). As components of Wnt signaling are being actively pursued, the regulatory controls operating on this important developmental pathway remain to be established. The focus of the present study is to determine the role of sFRP1, a Wnt antagonist whose activity will affect both the canonical and non-canonical pathways, during embryonic and post-natal development.

Inactivation and attenuation of Wnt signaling is regulated by several classes of secreted antagonists that include secreted frizzled-related proteins (sFRP) including sFRP1 to 5 (also known as secreted apoptosis related factors), Sizzled and Crescent (Kawano and Kypta, 2003; Lee et al., 2006), Wnt inhibitory factors (WIFs) and Cerberus by binding to Wnt, as well as Dickkopf which binds to the low density lipoprotein receptor related protein (LRP5) Wnt co-receptor and specifically inhibits canonical Wnt signaling (He et al., 2004). Dkk2 was recently shown to have a critical role in regulating mineralization of the bone matrix, highlighting the significance of regulating Wnt signaling in the skeleton (Li et al., 2005). The sFRPs are soluble ~314 amino acid proteins and have a cysteine-rich (CRD) domain similar to FZD receptors for binding to Wnt ligands (Kawano and Kypta, 2003). Expression of sFRPs are either overlapping or are relatively tissue restricted (Melkonyan et al., 1997; Hoang et al., 1998; Leimeister et al., 1998; Terry et al., 2000) and can provide distinct functional activities with specific Wnt ligands (Dennis et al., 1999; Galli et al., 2006). Because both sFRP1 and sFRP2 overlap in expression in many tissues and mice null for each of these sFRPs are viable, a double homozygous knockout was recently characterized which resulted in a lethal embryonic phenotype (E16.5) with reduction of the anterior-posterior axis, incomplete somite segmentation and digit and hindlimb abnormalities (Satoh et al., 2006). Embryos carrying the triple mutation for sFRP1, sFRP2, and sFRP5 have also been shown to be lethal at E12.5, with severe axis patterning defects (Satoh et al., 2008).

The biological relevance of the sFRP1 Wnt antagonist is known for many tissues. sFRP1 has established roles during the formation of neovessels (Goodwin and d'Amore, 2002), in the eye and for retinal cell differentiation (Kim et al., 2007), during cardiomyogenesis and hematopoiesis (Naito et al., 2006; Kwon et al., 2007), and in the adult skeleton in regulating Runx2 for chondrocyte hypertrophy, osteoblast differentiation and osteocyte apoptosis (Bodine et al., 2004; Gaur et al., 2005, 2006). sFRP1 regulates cell proliferation in different tissues including the proliferative zone of developing neurons (Augustine et al., 2001), for growth control of endothelial cells (Duplaa et al., 1999) and mesenchymal osteoprogenitors (Bodine et al., 2004; Gaur et al., 2005, 2006). sFRP1 is highly expressed in the kidney (Leimeister et al., 1998; Yoshino et al., 2001) and its loss is associated with renal cell carcinoma (Dahl et al., 2007; Huang et al., 2007; Gumz et al., 2007). Importantly, enhanced Wnt signaling in the sFRP1 null mouse delays the onset of age-dependent trabecular bone

loss (Bodine et al., 2004). Recently SFRP1 has been linked to several cancers through either epigenetic silencing or chromosome deletions (Takada et al., 2004; Gumz et al., 2007).

The importance of canonical Wnt signaling for regulation of skeletal development and bone formation in the adult is well documented (reviewed in Church and Francis-West, 2002; Bodine and Komm, 2006; Krishnan et al., 2006). Significantly, mutations in the LRP5 gene encoding the Wnt co-receptor first identified canonical Wnt signaling as a key regulator of bone mass. Loss-of-function characterized osteoporosis-pseudoglioma, while an activating mutation was found to increase bone mass in human and in mouse models (reviewed in Bodine and Komm, 2006). Furthermore, Wnt signaling is a normal physiologic and anabolic response to mechanical loading in the skeleton (Robinson et al., 2006; Sawakami et al., 2006). The essential role of canonical Wnt signaling for embryonic bone development was emphasized by conditional genetic modifications in β-catenin expression, which demonstrated that the level of β-catenin activity regulates progenitor cell commitment to either chondrocytes or osteoblasts for skeletal development (Day et al., 2005; Hill et al., 2005; Holmen et al., 2005). In vitro studies show expression of a broad array of the Wnt family members in differentiating osteoblasts and chondrocytes and that their activity requires regulation by Wnt antagonists, including sFRPs for normal cell growth and differentiation (Vaes et al., 2002; Bodine et al., 2005; Gaur et al., 2005, 2006; Baksh and Tuan, 2007).

Although sFRP1 is well known to act as an inhibitor of Wnt signaling, very little is known related to its requirement for embryonic development and post natal growth of the tissues in which it is expressed. Here we report the expression profile of sFRP1 reflected by LacZ gene expression in the sFRP1 gene knock-out mouse during embryonic and post-natal development. We observe normal development of the skeleton and soft tissues, except for the kidney beginning at the F8 generation. Our key findings are (1) robust β-gal activity, reflecting sFRP1 expression, occurs in osteoblasts in the embryonic skeleton of the $sFRP^{-/-}$ mouse; but after birth sFRP1 is only in osteoclasts, (2) sFRP1 expression is prominent in calvaria and limbs at the mineralizing front of bone formation during embryonic development, and (3) an increase in bone volume that can be observed in mice several weeks after birth. Importantly, ablation of sFRP1 does not lead to developmental abnormalities, impaired growth in the adult, or tumor formation in the $sFRP1^{-/-}$ mouse up to 2 years of age.

Materials and Methods

Animals

The sFRP1 knockout mice ($sFRP^{-/-}$) were produced by Lexicon Genetics, Inc. (The Woodlands, TX) as previously described (Bodine et al., 2004). The LacZ gene was inserted in place of exon 1 of the sFRP1 gene so that promoter activity could be followed by β-gal expression in $sFRP1^{-/-}$ mice. WT and homozygous knockout lines in C57BL/6 background strain were maintained at the University of Massachusetts by IACUC approved procedures. Genotyping was carried out as previously described (Bodine et al., 2004). In our facility, mice exhibited similar growth and life span as reported earlier (Bodine et al., 2004).

β-gal activity

All embryos, bone and soft tissues were fixed in 2% paraformaldehyde with 0.2% glutaraldehyde and containing 5 mM EGTA (pH 7.3), 2 mM $MgCl_2$, all in 1X PBS pH 8.8 at 4°C (Mundlos et al., 1997). Fixation times varied from 2 to 6 h for embryos d 11.5–15.5 at 4°C. Embryos d 16.5–19.5 and bones of post natal mice were fixed overnight at 4°C under vacuum. The standard staining reagent [5 mM Potassium Ferricyanide, 5 mM Potassium Ferrocyanide (Sigma-Aldrich, St. Louis, MO), 2 mM $MgCl_2$ (Fischer, Fairlawn, NJ), 0.2% NP-40 (United States Biomedical, Cleveland, OH), 0.01% Na-deoxycholate (Sigma), 1 mg/ml X-gal (Gold Biotechnology, St. Louis, MO), made up in 1× PBS (pH 7.2)] was used. Embryos and dissected tissue were rinsed in and equilibrated in 3% DMSO to prevent non-specific staining from developing upon storage in PBS. After β-gal staining, embryos were equilibrated in 30% sucrose (pH 7.4) and embedded in OCT (Triangle Biomedical Sciences, Durham, NC) for cryosectioning. Sections were restained for β-gal at room temperature overnight or alternatively 4–6 h at 37°C. To detect specific β-gal staining in intestine and osteoclasts of E17.5 or newborn, intestine and limbs were dissected, fixed and frozen sectioned prior to staining for only 30 min to 1 h when β-gal activity was detected in KO, and not in WT.

Histology, skeletal staining and bone density procedures

Frozen sections (12–20 μm) were obtained with a bright/Hacker (model OTF) Instrument (Fairfield, NJ), The CryoJane (Hackensack, NJ), tape transfer was used on bone sections (Instrumedics, Hackensack, NJ). Serial cryosections of embryos and newborn pups were also stained either with hematoxylin and eosin or eosin only for β-gal stained sections, safranin-O to visualize cartilage tissue or alkaline phosphatase enzyme activity to detect osteoblasts and bone formation activity using Sigma Aldrich reagents AS-MX disodium salt and Fast Red salt according to the procedure described in Lengner et al. (2004). Toluidine blue and von Kossa silver stains were combined for identifying cartilage and mineralized tissue. For paraffin sectioning bone from post-natal ages, demineralization was performed with neutral 18% EDTA for several days, followed by H&E or Toluidine blue staining was performed for cellular detail. Plastic (JB-4 methacrylate, Polysciences, Warrington, PA) embedment was used for sectioning un-demineralized bone at 4 weeks age. Sections were imaged with a CCD camera from either a dissecting microscope (Leica MZ7.5, Switzerland) or light microscope (Zeiss, Axioplan, Germany). We thank Joseph Grande, Department of Pathology and Rajiv Kumar, Department of Internal Medicine, Mayo Clinic, Rochester MN 55905 for their evaluation of the kidney phenotype. Alizarin red and Alcian blue stained skeletons were prepared by standard procedures (Lufkin et al., 1992).

Radiography of embryos, post-natal mice and dissected limbs was performed at 22 kv using a Faxitron (Wheeling, IL). Bone mineral density was obtained by DEXA measurements (P1X1Mus, GE-Lunar Corp., Madison, WI) on 4 weeks age femurs. Bones were first dissected and cleaned from adherent tissue, then fixed in 3.8% paraformaldehyde then analyzed per group of n = 3 WT and KO males among different litters.

RNA isolation and Northern blot analyses

Total RNA was isolated from tissues using Trizol reagent according to the manufacturer's instructions (GIBCO Invitrogen, Gaithersburg, MD). Northern hybridization was performed as previously described (Shalhoub et al., 1991) or quantitative PCR using primers for sFRP1 from Applied Biosystems (Foster City, CA) and SYBR-Green master mix as detailed elsewhere (Gaur et al., 2006). A 379 bp sFRP-1cDNA fragment from the CRD was generated by PCR using the following primers (forward 5′-CGGCCAGCGAGTACGACT ACGTGAGC-3′, reverse 5′-GCATCTCGGGC CAGATAGAAGCCGAAG-3′) for northern analyses which was performed with 10 μg of total RNA. RNA samples (10 μg) were electrophoresed in 1% formaldehyde-agarose gels and transferred to Hybond-N+ membrane (Amersham Pharmacia Biotech, Arlington Heights, IL) in 20× SSC (0.15 M NaCl, 0.015 sodium citrate). Blots were hybridized with randomly primed (Prime-It Kit, Strategene, La Jolla, CA), ^{32}P labeled cDNA probe for sFRP1. Blots were stripped and reprobed for GAPDH.

Ex vivo osteoblast and osteoclast studies

Osteoblasts were isolated from 2-day-old wild-type or knockout pups. Calvaria were excised, suture tissue removed and minced bone tissue from parietal and frontal segments were subjected to three rounds (5, 8, and 40 min) of digestion with Collagenase P (Roche Applied Science, Indianapolis, IN) at 37°C. The osteoblasts were obtained from third digestion mix, resuspended in α-MEM supplemented with 10% FBS and plated in 12-well plates at the density of 75,000 cell per well.

After reaching confluence, cells were differentiated towards osteogenesis in BGJb medium supplemented with 10% FBS, 50 μg/ml ascorbic acid and 10 mM β-glycerol phosphate. The medium was changed every second day. For every time point harvested, cells were fixed for 10 min with 0.5% glutaraldehyde (Electron Microscopy Sciences, Hatfield, PA) for LacZ staining or with 2% paraformaldehyde for AP and von Kossa staining. Cellular DNA synthesis was measured by [^{3}H]-thymidine incorporation is previously described (Stein et al., 1994).

Osteoclasts were generated from bone marrow of BalbC mice as previously described (Saltman et al., 2005). Briefly control and RANKL treated cells (4 ng/ml recombinant purified from R&D Systems, Minneapolis, MN) were collected after 4 days for RNA isolation and quantitative PCR detection of sFRP1.

Results

Restricted expression of sFRP1 in soft tissues and developing limb structures during embryonic development

We addressed tissue distribution of sFRP1, reflected by activity of its endogenous promoter that is monitored by β-gal enzyme detection during embryonic development in the homozygous mutant mouse carrying the knock in mutation of the sFRP1 gene schematically illustrated in Figure 1A. Northern blot analysis of whole embryo total RNA tissue using sFRP1 cDNA as probe, demonstrated that sFRP1 expression is observed at significant levels

at E11 (Fig. 1B). The sFRP1 mRNA levels in whole embryo decline relative to increasing embryo age. Confirmation of ablation of a functional sFRP1 mRNA was obtained by analysis of limb bone and kidney in wild-type (WT) and homozygous null mice ($sFRP1^{-/-}$) age 10-day postnatal (Fig. 1C). Kidney is a tissue known to express high levels of sFRP1 and served as a positive control. In the WT ($sFRP1^{+/+}$), the relative level of sFRP1 expression in limb bone tissue is found to be far less than in kidney. In both tissues, a complete absence of sFRP1 is indicated in the sFRP1 knockout (KO) homozygous.

Whole embryos, homozygous for the sFRP1 null mutation, were stained for β-gal activity (Fig. 2). Expression is robust at E11.5 and occurs primarily in the frontal brain, the more cranial somites (regions of spinal ganglion formation) with weaker expression in the spine, the lower abdominal cavity and focal regions of the eye and ear by E 13.5 and this pattern of sFRP1 expression is specific (Fig. 2 compares E13.5 WT and KO). Beginning at E14.5 and through E16.5, β-gal activity is restricted in expression to brain, eye, lower abdomen and the upper spine. Beginning at E15.5, β-gal activity was observed in the developing axial skeleton, scapula and lower limb joints, shown for example between the ischmus and femur, the tibia and femur (Fig. 2). Not until E17.5 is β-gal activity robustly observed throughout the skeleton, in the limbs (Fig. 3A-a,b), bony portions of the ribs (Fig. 3A-c,d) and vertebrae bodies with robust expression at growth plates as shown for sterna vertebrae (Fig. 3A-e,f). At birth β-gal activity appears weak in calvaria (Fig. 3A-g,h), but robust in ossifying nasal bones (Fig. 3A-i). At birth β-gal activity was not observed in osteoblasts on cortical or trabecular bone. However, in several limbs, restricted regions of positive chondrocytes were found near the articular surface and near tendon insertion (Fig. 3B). Thus, sFRP1 expression in the skeleton is detected predominantly in embryos where new bone formation for all bones, at the growth plates, but not in mature cartilage tissue of the rib and between the vertebrae.

Organ development in $sFRP1^{-/-}$ (KO) mouse

To identify potential abnormalities in development of specific tissues expressing sFRP1, organs were removed from the post-natal mouse. Strong expression of sFRP1 continued after birth in brain, heart, kidneys (Fig. 4a,d,g), with less in spleen and absent in lung (not shown). Intestine was strongly positive, although controls exhibited non-specific intestinal staining (data not shown). The intensity of sFRP1 expression in the forebrain (frontal lobes and optical bulbs) continued until 3 weeks (Fig. 4b); however, hindbrain expression of sFRP1 was no longer evident. β-gal activity completely diminished in the frontal lobes in a 3-month brain (data not shown). In the heart, sFRP1 expression is observed in the entire atrium and the larger blood vessels of the heart (aorta, coronary arteries, cardiac veins) surrounding the ventricle (Fig. 4d,e). No β-gal activity was detected 1 week after birth (data not shown).

In the kidney of the newborn, a uniform sFRP1 expression pattern was observed (Fig. 4g). This expression was retained through 2 months age in KO mice, while WT kidney remained negative. The visible structures observed in whole tissue are identified in frozen sections as tubules in the kidney cortex (Fig. 4h). No β-gal positive cells were associated with glomeruli structures. Kidneys were thoroughly examined at several post-natal ages up to 1 year

(Bodine et al., 2004) and no abnormalities were found up to 5 years of breeding. Beginning in the F8 generation (year 2005), we observed a mild phenotype in only four KO mice (Fig. 5). In two mice from 9 KO litters examined at birth, paraffin sections showed that kidney organization of the cortex appears similar between WT and KO, but medulla and renal papilla morphology differ (Fig. 5A–C). Medullary rays are not well defined and the papilla appeared reduced in size. At higher magnification, tubules and collecting ducts express sFRP1 (Fig. 5C). In another litter at 4 weeks age, two KO mice were observed with slightly larger kidneys having diminished cortex and increased medulla area (Fig. 5D). At higher magnification (Fig. 5E), collecting tubules and distal convoluted tubule cells appeared vacuolated and swollen in the KO mouse. In 2007 (F12 generation) we observed this phenotype in 4 from 40 male mice (2 at 4 weeks age/10 mice; 2 at 12 weeks age/30 mice). A higher density of glomeruli was again found in the cortex and at the corticomedullary junction in SFRP1$^{-/-}$ mouse compared to the WT mouse (Fig. 5F). Thus the frequency of occurrence of these kidney changes may become more manifest in later generations, although none of our sFRP$^{-/-}$ homozygous breeders of the F8–F12 generations which were sacrificed at 8 months exhibited enlarged kidneys.

Alizarin red/Alcian blue staining revealed the presence of all skeletal elements and normal bone and cartilage structures at birth in the KO (Fig. 6A). Skeletal X-rays also indicated similar pattern formation, sizes and density of individual bones in the newborn between WT and KO (data not shown). Histology of the limbs at birth showed normal growth plate organization, cortical thickness, but a suggestion of increased trabecular bone formation by ~21% increase in von Kossa staining that was more apparent with increasing age (Fig. 6B). This was consistent in sections throughout the depth of bone KO femurs. No significant differences were found in post-natal weight or body length monitored up to 4 weeks or in mouse activity examined for up to a year (data not shown) between sFRP1 WT and KO mice. We conclude from these findings, that ablation of the sFRP1 does not result in abnormalities in soft tissues or the skeleton that would compromise embryonic development which depends on Wnt signaling.

Skeletal expression of sFRP1 is transient and related to ossification

Previous studies examined sFRP1 expression in mouse embryos by in situ hybridization, but only from E7 to E10 prior to bone tissue formation and (Hoang et al., 1998). We examined frozen sections of the sFRP1$^{-/-}$ mouse embryo from E 14.5 to newborn to reveal a more accurate distribution of sFRP1 expression throughout the skeleton. We observed intense β-gal activity from E17.5 (Fig. 7A) to birth (Fig. 7B) during formation of the endochondral bones. At E17.5 sFRP1 expression occurs in the regions undergoing endochondral ossification overlapping areas of alkaline phosphatase activity (Fig. 7A, rib cross-section). In the longitudinal section of the bony part of the rib (shown in Fig. 7A), β-gal positive cells coincide with cortical bone formation. Expression of sFRP1 expression remained prominent at birth in the limbs, vertebrae, ribs, and the intramembranous craniofacial bones (peripheral regions of the calvaria, mandible and maxilla) (Fig. 7B, newborn). Comparing serial sections of embryos by β-gal staining and by alkaline phosphatase (AP) activity, again identifies the strongest sFRP1 expression overlapping the most intensely stained areas of bone formation (i.e., AP activity) showing two examples (Fig. 7C), the jaw bone and

vertebrae sections at higher magnification. Therefore, the robust β-gal activity we observe in bone tissue in the newborn and in the younger E15.5 embryo (see Fig. 3) indicate that sFRP1 is expressed during bone formation with mineral deposition.

To further address the relationship between sFRP1 expression and the onset of new bone formation, calvarial tissue was examined for sFRP1 expression during intramembranous bone formation (Fig. 8). At embryonic age 16.5 dpc (Fig. 8A). β-gal staining in the forebrain is clearly distinct from the dura mater underlying the calvarium. This region of β-gal activity partially overlaps the region of alkaline phosphatase expression of the developing bone tissue. In the newborn (Fig. 8B), the β-gal positive region of the calvaria is markedly reduced but overlaps in part the alkaline phosphatase positive cells, which represents active mineral deposition in newly synthesized bone matrix.

In conclusion, sFRP1 promoter activity (β-gal staining) is detected in the skeleton at maximal levels in bone tissue from E16.5 to prior to birth. This expression occurs in relation to the alkaline phosphatase positive bone forming front in both intramembranous and endochondral bone tissues. Finally, normal bone development is not compromised by the sFRP1 null mutation during the embryonic period, and the only change observed at birth is an apparent increase in trabecular bone from von Kossa stained histological sections.

Ex vivo derived calvarial osteoblasts from the sFRP1 null mouse exhibit a mild phenotype

Our results indicate that sFRP1 is expressed in osteoblasts with the onset of calcified tissue formation in both intramembranous and endochondral bone formation (see Figs. 3 and 8). The cellular transitions from the preosteoblast to osteoblast and osteocyte are fundamental to formation of normal bone in vivo. Therefore to assure that a potential osteoblast phenotype was not overlooked in skeletal and histologic sections, osteoblasts were isolated from the calvaria of neonatal WT and KO mice. For each experiment, we used pups from one entire litter to minimize pool effects due to interlitter variation. Cells harvested from the central bone areas of the KO did not express significant β-gal activity until confluency when they are differentiated and express alkaline phosphatase (Fig. 9A, day 10). In independent experiments examining cells by histochemical staining at different stages, we consistently find that the sFRP1$^{-/-}$ osteoblasts (β-gal positive) exhibit more robust alkaline phosphatase (AP) staining a few days earlier than cells from the WT mouse, as well as accelerated differentiation (increased mineral deposition) through the matrix maturation stage up to day 14. During the mineralization stage of differentiation (onset days 13–14 in WT), significant differences in AP and mineral staining are not observed through day 21 (data not shown). However, in the late differentiation stage (heavily mineralized cultures) (Fig. 9A, day 26), we find that AP is downregulated in the WT as expected with increased mineralization of the ECM (von Kossa stain), but AP enzyme activity continues to be maintained in KO cells. In addition, β-gal activity becomes downregulated, consistent with the absence of β-gal activity in mature calvarial bone of the day 3 KO mouse. These findings show that absence of sFRP1 in osteoprogenitors leads to earlier differentiation of mature osteoblasts and potentially a delay in the final stage of maturation due to sustained activity of the osteoblasts in the late mineralization stage.

To better understand the positive effects of activation of Wnt signaling in the sFRP1$^{-/-}$ osteoblast on osteoblast differentiation, proliferation studies were performed. We observe a twofold increase in cell proliferation by ^{3}H thymidine uptake and a more modest effect by BrdU incorporation in KO cells compared to WT during log phase growth (Fig. 9B). Thus, the accelerated differentiation of sFRP1$^{-/-}$ cells appears to relate to an increase in growth rate with more cells reaching confluency and producing matrix sooner than WT, resulting in earlier induction of alkaline phosphatase and mineral deposition. In summary, these ex vivo studies provide one mechanism for the observed in vivo findings of enhanced bone formation in the post-natal KO mouse that further links sFRP1 function to the control of cell proliferation. No evidence of bone tumors was ever observed in studies up to a year. We conclude that in bone tissue, sFRP1 loss-of-function results in an anabolic outcome.

sFRP1 may function in bone remodeling

An earlier study showed that antibody or siRNA inhibition of sFRP1 enhanced, while recombinant sFRP1 could inhibit, osteoclast formation by binding to RANKL, the essential inducer for fusion of mononuclear cells leading to osteoclast differentiation (Hausler et al., 2004). We therefore first examined if osteoclast activity monitored by Tartrate-resistant acid phosphatase (TRAP) staining was altered in the sFRP1 null mouse. Newborn femurs did not reveal any difference in TRAP activity between the WT and KO mouse (Fig. 10). Post-natal bone at 1 week also did not show differences (data not shown). A typical example from different litters stained at the same time and compared throughout multiple sections of the samples is shown in Figure 10A. We next addressed if osteoclasts express sFRP1 specifically by examining β-gal activity in bone sections (Fig. 10B) and quantitating sFRP1 mRNA levels in osteoclasts formed in vitro (Fig. 10C). β-gal positive osteoclasts were observed in the KO bone and a single osteoclasts at high magnification shows β-gal positive multiple nuclei. The eosin counterstain shows an absence of β-gal nuclear staining in surrounding cells. To identify a functional activity of sFRP1 in relation to osteoclast differentiation, sFRP1 expression was examined in hematopoietic bone marrow cells in the absence and presence of RANKL (Fig. 10C, left part). After 4 days, RANKL treated cultures represented largely differentiated osteoclasts which were reduced 50% in sFRP1 expression normalized to GAPDH compared to the untreated monocytic precursors. To appreciate the contribution of sFRP1 to regulation of Wnt signaling in different bone cell population, we compared in the same Q-PCR analyses, sFRP1 levels adherent to bone marrow cells, among osteoclasts, and osteoblasts (Fig. 10C, right part). The very low expression of sFRP1 in osteoclasts and modest level in osteoblasts relative to hematopoietic cell-enriched bone marrow may explain why bone formation and bone turnover is not compromised in the sFRP1 mouse at birth.

We next examined long bone of 28-day male mice for changes in morphology. Radiography revealed increased density of the metaphysis (Fig. 11A). Histology reflected increased trabecular bone density and apparent thicker cortical bone (Fig. 11B). By negative imaging of von Kossa silver stained histologic sections, calcified areas of the femoral bone are better visualized (Fig. 11C). We quantitatively assessed mineral content of bone from WT and sFRP$^{-/-}$ femurs at 28 days by DEXA bone mineral density (Fig. 11C) which was increased by 18% for trabecular bone measured in the femur, consistent with radiography images,

however, statistical significance could not be achieved with n = 4 mice. Cortical vBMD was not affected. In summary, we conclude from these studies, that the sFRP null mouse exhibits a modest increase in Wnt signaling that results in anabolic effects on bone formation primarily in the metaphysis during the early post-natal growth period that is sustained throughout the lifespan of the mouse (Bodine et al., 2004).

Discussion

Several key findings are identified in the sFRP1 KO mouse from these studies that indicate a requirement for negative regulation of the Wnt pathway in the embryo and the adult, specifically by sFRP1. The overlap in expression patterns of sFRPs and particularly the functional redundancy of sFPR1 and sFRP2, both being required for late stage embryogenesis, has been elaborated (Leimeister et al., 1998; Satoh et al., 2006). Here, we find the expected patterns of sFRP1/β-gal activity in the young embryo (E11–16.5) consistent with previous reports (see Introduction Section), but also find significant changes in distribution of β-gal activity in the post-natal mouse in brain, eye, and the skeleton. Kidney and bone were examined in greater detail in these studies. We find expression in kidney proximal and distal tubules and collecting ducts in the embryo and post-natal mouse, but it is only after 5 years of breeding that a phenotype was observed with altered morphology of the tubules at the corticomedullary junction and in the medulla. While our previous studies documented that enhanced Wnt signaling due to gene inactivation of sFRP1 in this mouse model resulted in a higher bone mass in adult mouse (32 weeks), the present studies have addressed the contribution of sFRP1 to the developing skeleton. Significantly, we find a restricted profile of sFRP1 activity in the developing epiphysis at the articular surface and in bone tissue in relation to the mineralization front during endochondral and intramembranous bone formation. The present studies demonstrate that sFRP1 loss-of-function has no consequence on normal development and post-natal growth. Importantly our findings show that sFRP1 is transiently expressed in the skeletal cells during embryonic and post-natal development and establish that inhibition of sFRP1 has a mild anabolic effect on bone and osteoblast differentiation. Except for changes in the kidney in only a few mice, no major effects on organ development or post-natal activity are observed, nor does the $sFRP1^{-/-}$ mouse develop tumors examined over a 5-year period from initial characterization of the phenotype in sFRP1 mice. This observation was unexpected, given the linkage of loss-of-sFRP1 expression with various cancers (Joesting et al., 2005; Cowling et al., 2007; Gumz et al., 2007).

sFRP1 expression in soft tissues

The biological significance of sFRP1 expression in the developing embryo in our mouse model, in which the sFRP1 gene in its native location could be monitored by replacement of exon 1 with the LacZ reporter. Our studies are validated by the consistent expression profile of β-gal activity with patterns of sFRP1 mRNA expression reported by in situ hybridization. Prominent expression occurs primarily in the forebrain, midbrain, posterior eye structures, kidney, intestine (Hoang et al., 1998; Leimeister et al., 1998; Kim et al., 1999, 2001; Heller et al., 2002; Liu et al., 2003).

sFRP1 is expressed at high levels in embryonic metanephros and regulates kidney development (Lescher et al., 1998; Yoshino et al., 2001). In the rat metanephros, sFRP1 very specifically inhibits kidney tubule formation in organ culture (Yoshino et al., 2001). Yet, in the absence of sFRP1, kidney tissue structure is normal and was documented for many generations up to 1 year age (Bodine et al., 2004), Only in a few mice over 8 months old show hydronephrosis observed upon sacrifice of breeders. We examined systematically over a 1 year period kidney morphology at various ages and found that two KO litters (from 12 litters and n = 3 mice from 41 KO mice) exhibited a distinct change in tissue organization of the cortex and medulla, but no evidence of hydronephrosis. After 5 years of breeding (F12 generation), slightly enlarged kidneys were observed with increased frequency. A noticeable increase in glomeruli number was observed. Interestingly, β-gal activity was not observed in these structures and may have developed due to changes in the tubules and ducts. Additional studies would be required to appreciate the importance of these observations.

sFRP1 is expressed during heart morphogenesis and during neovessel formation and becomes undetectable in mature blood vessels (Ezan et al., 2004). Recent studies establish that canonical Wnt signaling promotes the expression of cardiac progenitors and their differentiation and that sFRP1 contributes to regulation of this role of Wnt signaling (Kwon et al., 2007). We observe intense staining in large vessels of the heart at birth which is consistent with high sFRP1/FrzA in endothelial cells (Ezan et al., 2004). We also observed sFRP1 expression in fine blood vessels in calvarial sutures and in the skin. β-gal activity in the spleen also reflects the pattern of fine capillaries. These findings are consistent with reports that sFRP1 controls vascular cell proliferation (Ezan et al., 2004; Wang et al., 2004; Bodine and Komm, 2006).

sFRP1 has a key role in eye development, in lens epithelial differentiation and Wnt signaling pathway in regulating the growth of retinal ganglion cell axons (Rodriguez et al., 2005; Kim et al., 2007). The eye orbit expresses all sFRPs; and thus the absence of sFRP1 has no obvious consequences on impaired vision. Furthermore, sFRP1 has not been linked to retinal abnormalities (Garcia-Hoyos et al., 2004) and we do not find the eye abnormalities described in the LRP5 Wnt co-receptor null mice (Bodine and Komm, 2006). Increased sFRP1 expression has been linked to intraocular pressure in glaucoma (Wang et al., 2008). Thus sFRP1 levels so strongly expressed in the eye orbit during development, may continue to function in the post-natal mouse.

sFRP1 expression by in situ hybridization had been characterized in the developing mouse cerebral neocortex and correlates to the generation of neurons for enlarging the cortical plate (Augustine et al., 2001). The sFPR1 expression we observe in the forebrain continues robustly after birth and may be important in adult life. sFRP1 can block dendritic development (Rosso et al., 2005) and upregulation of sFRP1 has been associated with brain tumors (Lee et al., 2003). We did not observe a change in daily activity of the KO mouse compared to WT that would suggest brain abnormalities.

sFRP1 activity in the skeleton

sFRP1 expression by in situ hybridization was reported during early embryogenesis in mesenchyme and cartilage elements of developing mouse and chick bone (Wada et al., 1999; Terry et al., 2000). Our studies show that in E15.5 to the newborn, a restricted and apparent transient expression of sFRP1 occurs. β-gal activity in cartilage tissue was not uniform, but most often in the epiphysis near the region of tendon insertion and/or the articular surface. Beyond the direct role of sFRP1 as a Wnt antagonist, it has been suggested that sFRPs may control morphogenetic gradients of Wnt activity or facilitate boundary definition of a developing tissue by reducing Wnt activity (Kawano and Kypta, 2003). The regional expression of sFRP1 in the epiphyses may reflect a contribution of sFRP1 to defining the articular cartilage surface and shape of the epiphysis. However epiphysis development and joint formation are normal in the KO mouse, indicating sFRP1 redundant function in the epiphysis. Of interest, sFRP1 expression and inhibition of Wnt signaling by Dkk1 has been linked to inflammatory arthritis (Imai et al., 2006; Diarra et al., 2007). It is notable that sFRP1 activity is not observed in mature cartilage in the embryo, for example, in ribs. Intense staining at the growth plates was consistently observed in the embryo and may be in part contributed by recruitment of blood vessels in this region, essential for the process of endochondral bone formation and to mineral deposition (Enomoto-Iwamoto et al., 2002; Gaur et al., 2006).

Bone tissue develops with normal structural features of tissue organization for endochondral and intramembranous bone. We have previously reported that the sFRPs 2–4 in bone are at normal levels in the KO (Bodine et al., 2004) and may have redundant functions with sFRP1; hence, developmental bone abnormalities are not observed in the embryonic skeleton in these studies. However, we clearly observe enhanced bone trabeculae in the KO mouse shortly after birth. At birth we cannot observe β-gal staining in active osteoblasts on the bone surface or in osteocytes in mineralized bone and this may be an issue of detection sensitivity. However, our ex vivo calvarial osteoblast studies provided insight into sFRP1 function and Wnt signaling requirements for embryonic bone formation in regulating cellular activity during active mineral deposition. The enhanced Wnt signaling in sFRP1$^{-/-}$ mice contributes to increasing the osteoprogenitor pool reflected by robust β-gal activity and increased DNA synthesis. The increased cell number leads to earlier confluence and multilayering that in turn enhances differentiation of sFRP1$^{-/-}$ osteoblasts. Studies in cell phenotypes have shown that increased sFRP1 expression correlates with control of cell proliferation (Melkonyan et al., 1997; Imai and D'Armiento, 2002; Ezan et al., 2004). sFRP1 may function then to regulate the growth of cells recruited into the osteoblast lineage. At the later stage of differentiation, β-gal activity is not present and we find stimulated osteoblast activity (AP staining) and less mineralization. Thus, sFRP1 function is important during osteoblast differentiation to attenuate Wnt signaling for progression to the osteocyte and a mature mineralized matrix. Notably, the highest sFRP1 expression in human osteoblast cell lines is found in pre-osteocytes (Bodine et al., 2005). These findings are consistent with ex vivo bone marrow stromal cell cultures isolated from 32-week-old mice (Bodine et al., 2004). Thus, sFRP1 functions to control cell number and fate of osteoblast sub-populations during development and in the adult skeleton and sFRP1 induces apoptosis of osteocytes in aging bone (Bodine et al., 2004).

A final consideration for sFRP1 activity in bone may be in contributing to control of bone turnover and not only bone formation as Wnt signaling influences osteoclastogenesis (Spencer et al., 2006). sFRP1 has been shown to bind to RANK ligand in osteoblasts and thereby inhibit osteoclast differentiation (Hausler et al., 2004). Our studies show a very low level of sFRP1 expression in osteoclasts compared to osteoblasts. Importantly, the absence of sFRP1 in osteoblasts has not compromised bone turnover and osteoclast number and activity (TRAP staining) appear to be equivalent.

Selective sFRP1 activity has been identified in various tissues/organs by our studies. In part this may be a consequence of sFRP1 interaction with specific Wnt ligands (Heller et al., 2002). sFRP1 selectively associates with Wnt1 in vascular endothelial cells and Wnt8 during heart morphogenesis (Dennis et al., 1999; Jaspard et al., 2000). Wnt5a and Wnt7a are broadly expressed in foregut mesenchyme starting around day 10 where we find strong sFRP1 expression (Dealy et al., 1993). Wnt9a maintains joint integrity (Spater et al., 2006). Wnt 14a induce synovial joint formation, a region where we find transient expression (Hartmann and Tabin, 2001). Later, Wnt-5A becomes localized at the perichondrium of bone precursors. Wnt10b maintains bone mass (Bennett et al., 2005), a phenotype observed in the $sFRP^{-/-}$ mice. The selective expression of sFRP1 we observe in the developing embryo in skeletal elements raises speculation as to specificity for sFRP1 interaction with particular Wnts, which are also expressed in distinct regions of the skeleton. For example, only sFRP1 and sFRP2 will antagonize Wnt3a (Galli et al., 2006; Wawrzak et al., 2007). Thus both selective and redundant regulation of Wnt signaling for different tissues is supported by sFRP1 and other inhibitors of the Wnt pathway.

In summary, there is an absence of remarkable abnormalities in the $sFRP1^{-/-}$ mouse, except for infrequent kidney changes after many generations of breeding KO mice. The normal developing embryo and the mild skeletal phenotype in the growing post-natal mouse reflected by a mild increase in trabecular and cortical bone mass indicates an advantage to the bone by reduction of sFRP1 levels. Recently, the increase in bone mineral density in the sFRP1 null mouse was found to be as effective as the anabolic effects of parathyroid hormone administration to the mouse (Bodine et al., 2007). The present studies characterizing normal development of the mouse embryo in the absence of a functional sFRP1 Wnt antagonist, coupled with the observed phenotype in aging mouse that results in a delay in bone loss, suggests that strategies to target sFRP1 inhibition have great promise as a therapeutic for treating osteoporosis, potentially without having effects on non-skeletal tissues.

Acknowledgments

We are indebted to Dr. Joseph Grande, Department of Pathology and Dr Rajiv Kumar (Mayo Clinic, Rochester MN 55905) for their evaluation of the kidney sections of the KO and WT mice and helpful discussions for future studies. J. Symons contributed to this study in partial fulfillment of the Bachelor of Science degree, Worcester Polytechnic Institute. We thank Judy Rask and Charlene Baron for manuscript preparation. This work was supported by a research grant to the University of Massachusetts Medical School from the Wyeth Research Women's Health and Musculoskeletal Biology, Collegeville, PA, and NIH grant AR039588.

Literature Cited

Augustine C, Gunnersen J, Spirkoska V, Tan SS. Place- and time-dependent expression of mouse sFRP-1 during development of the cerebral neocortex. Mech Dev. 2001; 109:395–397. [PubMed: 11731256]

Baksh D, Tuan RS. Canonical and non-canonical wnts differentially affect the development potential of primary isolate of human bone marrow mesenchymal stem cells. J Cell Physiol. 2007; 212:817–826. [PubMed: 17458904]

Behrens J, von Kries JP, Kuhl M, Bruhn L, Wedlich D, Grosschedl R, Birchmeier W. Functional interaction of beta-catenin with the transcription factor LEF-1. Nature. 1996; 382:638–642. [PubMed: 8757136]

Bennett CN, Longo KA, Wright WS, Suva LJ, Lane TF, Hankenson KD, MacDougald OA. Regulation of osteoblastogenesis and bone mass by Wnt10b. Proc Natl Acad Sci USA. 2005; 102:3324–3329. [PubMed: 15728361]

Bodine PV, Komm BS. Wnt signaling and osteoblastogenesis. Rev Endocr Metab Disord. 2006; 7:33–39. [PubMed: 16960757]

Bodine PV, Zhao W, Kharode YP, Bex FJ, Lambert AJ, Goad MB, Gaur T, Stein GS, Lian JB, Komm BS. The Wnt antagonist secreted frizzled-related protein-1 is a negative regulator of trabecular bone formation in adult mice. Mol Endocrinol. 2004; 18:1222–1237. [PubMed: 14976225]

Bodine PV, Billiard J, Moran RA, Ponce-de-Leon H, McLarney S, Mangine A, Scrimo MJ, Bhat RA, Stauffer B, Green J, Stein GS, Lian JB, Komm BS. The Wnt antagonist secreted frizzled-related protein-1 controls osteoblast and osteocyte apoptosis. J Cell Biochem. 2005; 96:1212–1230. [PubMed: 16149051]

Bodine PV, Seestaller-Wehr L, Kharode YP, Bex FJ, Komm BS. Bone anabolic effects of parathyroid hormone are blunted by deletion of the Wnt antagonist secreted frizzled-related protein-1. J Cell Physiol. 2007; 210:352–357. [PubMed: 17044082]

Church VL, Francis-West P. Wnt signalling during limb development. Int J Dev Biol. 2002; 46:927–936. [PubMed: 12455630]

Cowling VH, D'Cruz CM, Chodosh LA, Cole MD. c-Myc transforms human mammary epithelial cells through repression of the Wnt inhibitors DKK1 and SF RP1. Mol Cell Biol. 2007; 27:5135–5146. [PubMed: 17485441]

Dahl E, Wiesmann F, Woenckhaus M, Stoehr R, Wild PJ, Veeck J, Knuchel R, Klopocki E, Sauter G, Simon R, Wieland WF, Walter B, Denzinger S, Hartmann A, Hammerschmied CG. Frequent loss of SFRP1 expression in multiple human solid tumours: Association with aberrant promoter methylation in renal cell carcinoma. Oncogene. 2007; 26:5680–5691. [PubMed: 17353908]

Day TF, Guo X, Garrett-Beal L, Yang Y. Wnt/beta-catenin signaling in mesenchymal progenitors controls osteoblast and chondrocyte differentiation during vertebrate skeletogenesis. Dev Cell. 2005; 8:739–750. [PubMed: 15866164]

Dealy CN, Roth A, Ferrari D, Brown AM, Kosher RA. Wnt-5a and Wnt-7a are expressed in the developing chick limb bud in a manner suggesting roles in pattern formation along the proximodistal and dorsoventral axes. Mech Dev. 1993; 43:175–186. [PubMed: 8297789]

Dennis S, Aikawa M, Szeto W, d'Amore PA, Papkoff J. A secreted frizzled related protein, FrzA, selectively associates with Wnt-1 protein and regulates wnt-1 signaling. J Cell Sci. 1999; 112:3815–3820. [PubMed: 10523516]

Diarra D, Stolina M, Polzer K, Zwerina J, Ominsky MS, Dwyer D, Korb A, Smolen J, Hoffmann M, Scheinecker C, van der HD, Landewe R, Lacey D, Richards WG, Schett G. Dickkopf-1 is a master regulator of joint remodeling. Nat Med. 2007; 13:156–163. [PubMed: 17237793]

Duplaa C, Jaspard B, Moreau C, d'Amore PA. Identification and cloning of a secreted protein related to the cysteine-rich domain of frizzled. Evidence for a role in endothelial cell growth control. Circ Res. 1999; 84:1433–1445. [PubMed: 10381896]

Eaves CJ. Manipulating hematopoietic stem cell amplification with Wnt. Nat Immunol. 2003; 4:511–512. [PubMed: 12774072]

Enomoto-Iwamoto M, Kitagaki J, Koyama E, Tamamura Y, Wu C, Kanatani N, Koike T, Okada H, Komori T, Yoneda T, Church V, Francis-West PH, Kurisu K, Nohno T, Pacifici M, Iwamoto M.

The Wnt antagonist Frzb-1 regulates chondrocyte maturation and long bone development during limb skeletogenesis. Dev Biol. 2002; 251:142–156. [PubMed: 12413904]

Ezan J, Leroux L, Barandon L, Dufourcq P, Jaspard B, Moreau C, Allieres C, Daret D, Couffinhal T, Duplaa C. FrzA/sFRP-1, a secreted antagonist of the Wnt-Frizzled pathway, controls vascular cell proliferation in vitro and in vivo. Cardiovasc Res. 2004; 63:731–738. [PubMed: 15306229]

Galli LM, Barnes T, Cheng T, Acosta L, Anglade A, Willert K, Nusse R, Burrus LW. Differential inhibition of Wnt-3a by Sfrp-1, Sfrp-2, and Sfrp-3. Dev Dyn. 2006; 235:681–690. [PubMed: 16425220]

Garcia-Hoyos M, Cantalapiedra D, Arroyo C, Esteve P, Rodriguez J, Riveiro R, Trujillo MJ, Ramos C, Bovolenta P, Ayuso C. Evaluation of SFRP1 as a candidate for human retinal dystrophies. Mol Vis. 2004; 10:426–431. [PubMed: 15235574]

Gaur T, Lengner CJ, Hovhannisyan H, Bhat RA, Bodine PVN, Komm BS, Javed A, van Wijnen AJ, Stein JL, Stein GS, Lian JB. Canonical WNT signaling promotes osteogenesis by directly stimulating RUNX2 gene expression. J Biol Chem. 2005; 280:33132–33140. [PubMed: 16043491]

Gaur T, Lengner CJ, Hussain S, Trevant B, Ayers D, Stein JL, Bodine PVN, Komm BS, Stein GS, Lian JB. Secreted frizzled protein 1 regulates Wnt signaling for BMP2 induced chondrocyte differentiation. J Cell Physiol. 2006; 208:87–96. [PubMed: 16575902]

Goodwin AM, d'Amore PA. Wnt signaling in the vasculature. Angiogenesis. 2002; 5:1–9. [PubMed: 12549854]

Gumz ML, Zou H, Kreinest PA, Childs AC, Belmonte LS, LeGrand SN, Wu KJ, Luxon BA, Sinha M, Parker AS, Sun LZ, Ahlquist DA, Wood CG, Copland JA. Secreted frizzled-related protein 1 loss contributes to tumor phenotype of clear cell renal cell carcinoma. Clin Cancer Res. 2007; 13:4740–4749. [PubMed: 17699851]

Hartmann C, Tabin CJ. Wnt-14 plays a pivotal role in inducing synovial joint formation in the developing appendicular skeleton. Cell. 2001; 104:341–351. [PubMed: 11239392]

Hausler KD, Horwood NJ, Chuman Y, Fisher JL, Ellis J, Martin TJ, Rubin JS, Gillespie MT. Secreted frizzled-related protein-1 inhibits RANKL-dependent osteoclast formation. J Bone Miner Res. 2004; 19:1873–1881. [PubMed: 15476588]

He X, Semenov M, Tamai K, Zeng X. LDL receptor-related proteins 5 and 6 in Wnt/beta-catenin signaling: Arrows point the way. Development. 2004; 131:1663–1677. [PubMed: 15084453]

Heller RS, Dichmann DS, Jensen J, Miller C, Wong G, Madsen OD, Serup P. Expression patterns of Wnts, Frizzleds, sFRPs, and misexpression in transgenic mice suggesting a role for Wnts in pancreas and foregut pattern formation. Dev Dyn. 2002; 225:260–270. [PubMed: 12412008]

Hill TP, Spater D, Taketo MM, Birchmeier W, Hartmann C. Canonical Wnt/beta-catenin signaling prevents osteoblasts from differentiating into chondrocytes. Dev Cell. 2005; 8:727–738. [PubMed: 15866163]

Hoang BH, Thomas JT, Abdul-Karim FW, Correia KM, Conlon RA, Luyten FP, Ballock RT. Expression pattern of two Frizzled-related genes, Frzb-1 and Sfrp-1, during mouse embryogenesis suggests a role for modulating action of Wnt family members. Dev Dyn. 1998; 212:364–372. [PubMed: 9671940]

Holmen SL, Zylstra CR, Mukherjee A, Sigler RE, Faugere MC, Bouxsein ML, Deng L, Clemens TL, Williams BO. Essential role of beta-catenin in post natal bone acquisition. J Biol Chem. 2005; 280:21162–21168. [PubMed: 15802266]

Huang J, Zhang YL, Teng XM, Lin Y, Zheng DL, Yang PY, Han ZG. Down-regulation of SFRP1 as a putative tumor suppressor gene can contribute to human hepatocellular carcinoma. BMC Cancer. 2007; 7:126. [PubMed: 17626620]

Imai K, D'Armiento J. Differential gene expression of sFRP-1 and apoptosis in pulmonary emphysema. Chest. 2002; 121:7S. [PubMed: 11893652]

Imai K, Morikawa M, D'Armiento J, Matsumoto H, Komiya K, Okada Y. Differential expression of WNTs and FRPs in the synovium of rheumatoid arthritis and osteoarthritis. Biochem Biophys Res Commun. 2006; 345:1615–1620. [PubMed: 16735027]

Jaspard B, Couffinhal T, Dufourcq P, Moreau C, Duplaa C. Expression pattern of mouse sFRP-1 and mWnt-8 gene during heart morphogenesis. Mech Dev. 2000; 90:263–267. [PubMed: 10640709]

Joesting MS, Perrin S, Elenbaas B, Fawell SE, Rubin JS, Franco OE, Hayward SW, Cunha GR, Marker PC. Identification of SFRP1 as a candidate mediator of stromal-to-epithelial signaling in prostate cancer. Cancer Res. 2005; 65:10423–10430. [PubMed: 16288033]

Kawano Y, Kypta R. Secreted antagonists of the Wnt signalling pathway. J Cell Sci. 2003; 116:2627–2634. [PubMed: 12775774]

Kim IS, Otto F, Zabel B, Mundlos S. Regulation of chondrocyte differentiation by Cbfa1. Mech Dev. 1999; 80:159–170. [PubMed: 10072783]

Kim AS, Lowenstein DH, Pleasure SJ. Wnt receptors and Wnt inhibitors are expressed in gradients in the developing telencephalon. Mech Dev. 2001; 103:167–172. [PubMed: 11335128]

Kim HS, Shin J, Kim SH, Chun HS, Kim JD, Kim YS, Kim MJ, Rhee M, Yeo SY, Huh TL. Eye field requires the function of Sfrp1 as a Wnt antagonist. Neurosci Lett. 2007; 414:26–29. [PubMed: 17222974]

Krishnan V, Bryant HU, MacDougald OA. Regulation of bone mass by Wnt signaling. J Clin Invest. 2006; 116:1202–1209. [PubMed: 16670761]

Kuhl M. The WNT/calcium pathway: Biochemical mediators, tools and future requirements. Front Biosci. 2004; 9:967–974. [PubMed: 14766423]

Kuhl M, Geis K, Sheldahl LC, Pukrop T, Moon RT, Wedlich D. Antagonistic regulation of convergent extension movements in Xenopus by Wnt/beta-catenin and Wnt/Ca^{2+} signaling. Mech Dev. 2001; 106:61–76. [PubMed: 11472835]

Kwon C, Arnold J, Hsiao EC, Taketo MM, Conklin BR, Srivastava D. Canonical Wnt signaling is a positive regulator of mammalian cardiac progenitors. Proc Natl Acad Sci USA. 2007; 104:10894–10899. [PubMed: 17576928]

Lee Y, Miller HL, Jensen P, Hernan R, Connelly M, Wetmore C, Zindy F, Roussel MF, Curran T, Gilbertson RJ, McKinnon PJ. A molecular fingerprint for medulloblastoma. Cancer Res. 2003; 63:5428–5437. [PubMed: 14500378]

Lee HX, Ambrosio AL, Reversade B, De Robertis EM. Embryonic dorsal-ventral signaling: Secreted frizzled-related proteins as inhibitors of tolloid proteinases. Cell. 2006; 124:147–159. [PubMed: 16413488]

Leimeister C, Bach A, Gessler M. Developmental expression patterns of mouse sFRP genes encodingmembers of the secreted frizzled related protein family. Mech Dev. 1998; 75:29–42. [PubMed: 9739103]

Lengner CJ, Lepper C, van Wijnen AJ, Stein JL, Stein GS, Lian JB. Primary mouse embyronic fibroblasts: A model of mesenchymal cartilage formation. J Cell Physiol. 2004; 200:327–333. [PubMed: 15254959]

Lescher B, Haenig B, Kispert A. sFRP-2 is a target of the Wnt-4 signaling pathway in the developing metanephric kidney. Dev Dyn. 1998; 213:440–451. [PubMed: 9853965]

Li X, Liu P, Liu W, Maye P, Zhang J, Zhang Y, Hurley M, Guo C, Boskey A, Sun L, Harris SE, Rowe DW, Ke HZ, Wu D. Dkk2 has a role in terminal osteoblast differentiation and mineralized matrix formation. Nat Genet. 2005; 37:945–952. [PubMed: 16056226]

Liu H, Mohamed O, Dufort D, Wallace VA. Characterization of Wnt signaling components and activation of the Wnt canonical pathway in the murine retina. Dev Dyn. 2003; 227:323–334. [PubMed: 12815618]

Lufkin T, Mark M, Hart CP, Dolle P, LeMeur M, Chambon P. Homeotic transformation of the occipital bones of the skull by ectopic expression of a homeobox gene. Nature. 1992; 359:835–841. [PubMed: 1359423]

Melkonyan HS, Chang WC, Shapiro JP, Mahadevappa M, Fitzpatrick PA, Kiefer MC, Tomei LD, Umansky SR. SARPs: A family of secreted apoptosis-related proteins. Proc Natl Acad Sci USA. 1997; 94:13636–13641. [PubMed: 9391078]

Mundlos S, Otto F, Mundlos C, Mulliken JB, Aylsworth AS, Albright S, Lindhout D, Cole WG, Henn W, Knoll JHM, Owen MJ, Mertelsmann R, Zabel BU, Olsen BR. Mutations involving the transcription factor CBFA1 cause cleidocranial dysplasia. Cell. 1997; 89:773–779. [PubMed: 9182765]

Naito AT, Shiojima I, Akazawa H, Hidaka K, Morisaki T, Kikuchi A, Komuro I. Developmental stage-specific biphasic roles of Wnt/beta-catenin signaling in cardiomyogenesis and hematopoiesis. Proc Natl Acad Sci USA. 2006; 103:19812–19817. [PubMed: 17170140]

Nusse R. Wnt signaling in disease and in development. Cell Res. 2005; 15:28–32. [PubMed: 15686623]

Reya T, Duncan AW, Ailles L, Domen J, Scherer DC, Willert K, Hintz L, Nusse R, Weissman IL. A role for Wnt signalling in self-renewal of haematopoietic stem cells. Nature. 2003; 423:409–414. [PubMed: 12717450]

Robinson JA, Chatterjee-Kishore M, Yaworsky PJ, Cullen DM, Zhao W, Li C, Kharode Y, Sauter L, Babij P, Brown EL, Hill AA, Akhter MP, Johnson ML, Recker RR, Komm BS, Bex FJ. Wnt/beta-catenin signaling is a normal physiological response to mechanical loading in bone. J Biol Chem. 2006; 281:31720–31728. [PubMed: 16908522]

Rodriguez J, Esteve P, Weinl C, Ruiz JM, Fermin Y, Trousse F, Dwivedy A, Holt C, Bovolenta P. SFRP1 regulates the growth of retinal ganglion cell axons through the Fz2 receptor. Nat Neurosci. 2005; 8:1301–1309. [PubMed: 16172602]

Rosso SB, Sussman D, Wynshaw-Boris A, Salinas PC. Wnt signaling through Dishevelled, Rac and JNK regulates dendritic development. Nat Neurosci. 2005; 8:34–42. [PubMed: 15608632]

Saltman LH, Javed A, Ribadeneyra J, Hussain S, Young DW, Osdoby P, Amcheslavsky A, van Wijnen AJ, Stein JL, Stein GS, Lian JB, Bar-Shavit Z. Organization of transcriptional regulatory machinery in osteoclast nuclei: Compartmentalization of Runx1. J Cell Physiol. 2005; 204:871–880. [PubMed: 15828028]

Satoh W, Gotoh T, Tsunematsu Y, Aizawa S, Shimono A. Sfrp1 and Sfrp2 regulate anteroposterior axis elongation and somite segmentation during mouse embryogenesis. Development. 2006; 133:989–999. [PubMed: 16467359]

Satoh W, Matsuyama M, Takemura H, Aizawa S, Shimono A. Sfrp1, Sfrp2, and Sfrp5 regulate the Wnt/beta-catenin and the planar cell polarity pathways during early trunk formation in mouse. Genesis. 2008; 46:92–103. [PubMed: 18257070]

Sawakami K, Robling AG, Ai M, Pitner ND, Liu D, Warden SJ, Li J, Maye P, Rowe DW, Duncan RL, Warman ML, Turner CH. The Wnt co-receptor LRP5 is essential for skeletal mechanotransduction but not for the anabolic bone response to parathyroid hormone treatment. J Biol Chem. 2006; 281:23698–23711. [PubMed: 16790443]

Shalhoub V, Jackson ME, Lian JB, Stein GS, Marks SC Jr. Gene expression during skeletal development in three osteopetrotic rat mutations. Evidence for osteoblast abnormalities. J Biol Chem. 1991; 266:9847–9856. [PubMed: 2033073]

Spater D, Hill TP, O'sullivan RJ, Gruber M, Conner DA, Hartmann C. Wnt9a signaling is required for joint integrity and regulation of Ihh during chondrogenesis. Development. 2006; 133:3039–3049. [PubMed: 16818445]

Spencer GJ, Utting JC, Etheridge SL, Arnett TR, Genever PG. Wnt signalling in osteoblasts regulates expression of the receptor activator of NFkappaB ligand and inhibits osteoclastogenesis in vitro. J Cell Sci. 2006; 119:1283–1296. [PubMed: 16522681]

Stein, GS.; Stein, JL.; Lian, JB.; Last, TJ.; Owen, T.; McCabe, L. Synchronization of normal diploid and transformed mammalian cells. In: Celis, JE., editor. Cell Biology: A laboratory Handbook. San Diego, CA: Academic Press, Inc.; 1994. p. 282-287.

Takada T, Yagi Y, Maekita T, Imura M, Nakagawa S, Tsao SW, Miyamoto K, Yoshino O, Yasugi T, Taketani Y, Ushijima T. Methylation-associated silencing of the Wnt antagonist SFRP1 gene in human ovarian cancers. Cancer Sci. 2004; 95:741–744. [PubMed: 15471560]

Terry K, Magan H, Baranski M, Burrus LW. Sfrp-1 and sfrp-2 are expressed in overlapping and distinct domains during chick development. Mech Dev. 2000; 97:177–182. [PubMed: 11025221]

Vaes BLT, Dechering KJ, Feijen A, Hendriks JMA, Lefevre C, Mummery C, Olijve W, Van zoelen EJ, Steegenga WT. Comprehensive microarray analysis of bone morphogenetic protein 2-induced osteoblast differentiation resulting in the identification of novel markers for bone development. J Bone Miner Res. 2002; 17:2106–2118. [PubMed: 12469905]

Veeman MT, Axelrod JD, Moon RT. A second canon. Functions and mechanisms of beta-catenin-independent Wnt signaling. Dev Cell. 2003; 5:367–377. [PubMed: 12967557]

Wada N, Kawakami Y, Ladher R, Francis-West PH, Nohno T. Involvement of Frzb-1 in mesenchymal condensation and cartilage differentiation in the chick limb bud. Int J Dev Biol. 1999; 43:495–500. [PubMed: 10610022]

Wang HY, Malbon CC. Wnt signaling, Ca^{2+}, and cyclic GMP: Visualizing Frizzled functions. Science. 2003; 300:1529–1530. [PubMed: 12791979]

Wang X, Adhikari N, Li Q, Hall JL. LDL receptor-related protein LRP6 regulates proliferation and survival through the Wnt cascade in vascular smooth muscle cells. Am J Physiol Heart Circ Physiol. 2004; 287:H2376–H2383. [PubMed: 15271658]

Wang WH, McNatt LG, Pang IH, Millar JC, Hellberg PE, Hellberg MH, Steely HT, Rubin JS, Fingert JH, Sheffield VC, Stone EM, Clark AF. Increased expression of the WNT antagonist sFRP-1 in glaucoma elevates intraocular pressure. J Clin Invest. 2008; 118:1056–1064. [PubMed: 18274669]

Wawrzak D, Metioui M, Willems E, Hendrickx M, de GE, Leyns L. Wnt3a binds to several sFRPs in the nanomolar range. Biochem Biophys Res Commun. 2007; 357:1119–1123. [PubMed: 17462603]

Willert K, Brown JD, Danenberg E, Duncan AW, Weissman IL, Reya T, Yates JR III, Nusse R. Wnt proteins are lipid-modified and can act as stem cell growth factors. Nature. 2003; 423:448–452. [PubMed: 12717451]

Yoshino K, Rubin JS, Higinbotham KG, Uren A, Anest V, Plisov SY, Perantoni AO. Secreted Frizzled-related proteins can regulate metanephric development. Mech Dev. 2001; 102:45–55. [PubMed: 11287180]

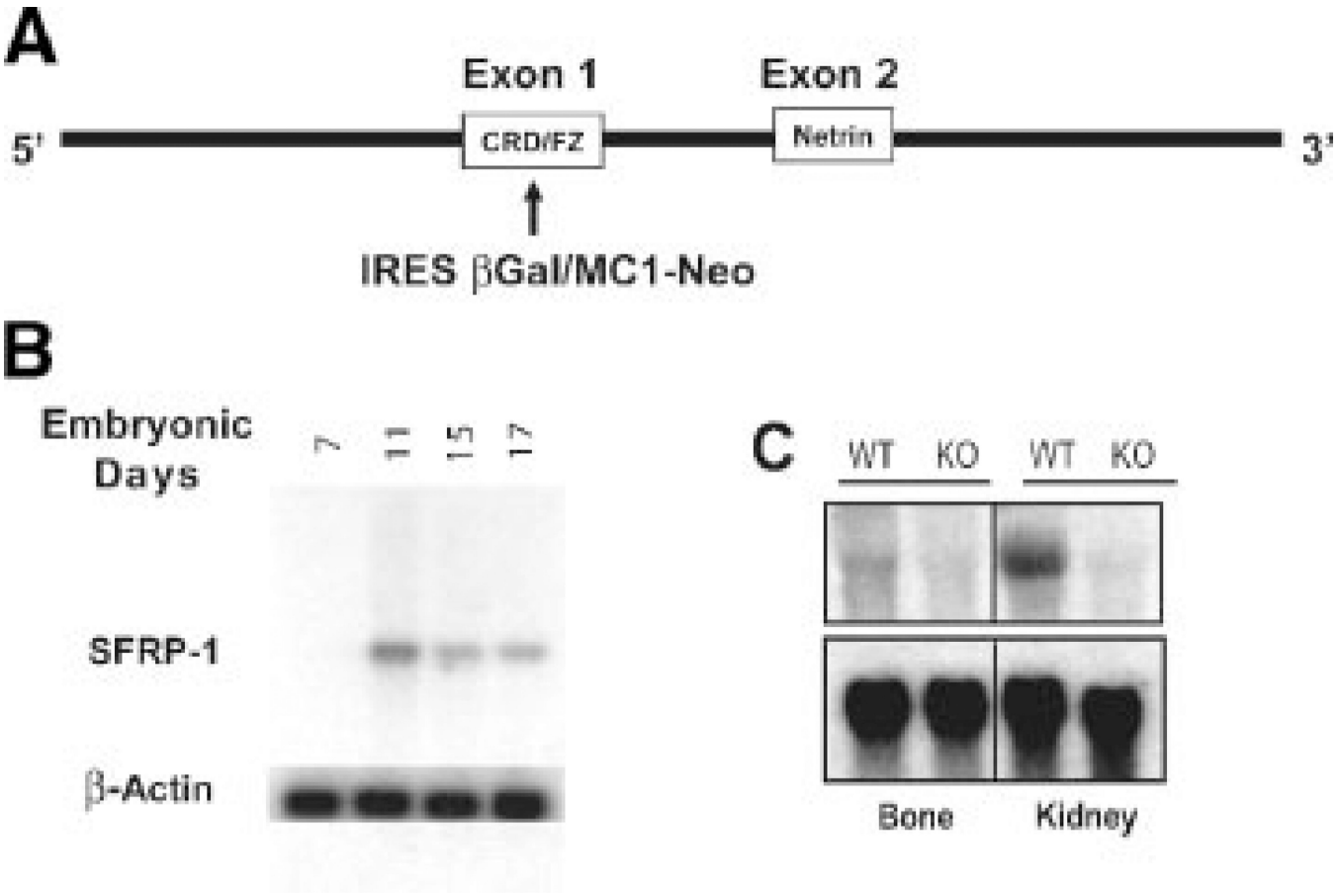

Fig. 1.

Ablation of sFRP1 in mouse. A: Schematic illustration of the knock-in mutation of the sFRP1 locus by insertion of LacZ/β-gal in exon 1 by homologous recombination. Two functional domains are indicated, the cysteine rich domain/frizzled receptor-like (CRD/FZ) and the netrin. A non-functional protein is generated by replacing the CRD/FZ domain which interacts with Wnt ligands. B: Northern analysis of whole embryo total cellular RNA from embryonic days E7 through E17 during the onset of formation of cartilaginous and osseous skeletal elements. C: Northern analysis of bone and kidney tissues (d10, post-natal) to show relative expression levels in WT (+/+) and validate the complete loss of sFRP1 mRNA expression in the sFRP1 KO mouse (−/−).

Fig. 2.

Expression of sFRP1 in the mouse embryo during development by β-gal activity. At the indicated ages, whole embryos were fixed and stained for β-gal activity as described in methods. Upper parts—selective expression in tissues by E11.5 in the brain, eye, caudal somites and in the abdominal cavity. At E13.5, epiphysis regions of the developing limbs (arrows) are also positive (arrows). An E13.5 sFRP1$^{+/+}$ control (WT) is shown to demonstrate normal development and that β-gal activity is specific. Lower parts—E15.5: Expression continues in the brain (frontal view), epiphysis (arrows and scapula in side view) and somites (lateral view). [Color figure can be viewed in the online issue, which is available at www.interscience.wiley.com.]

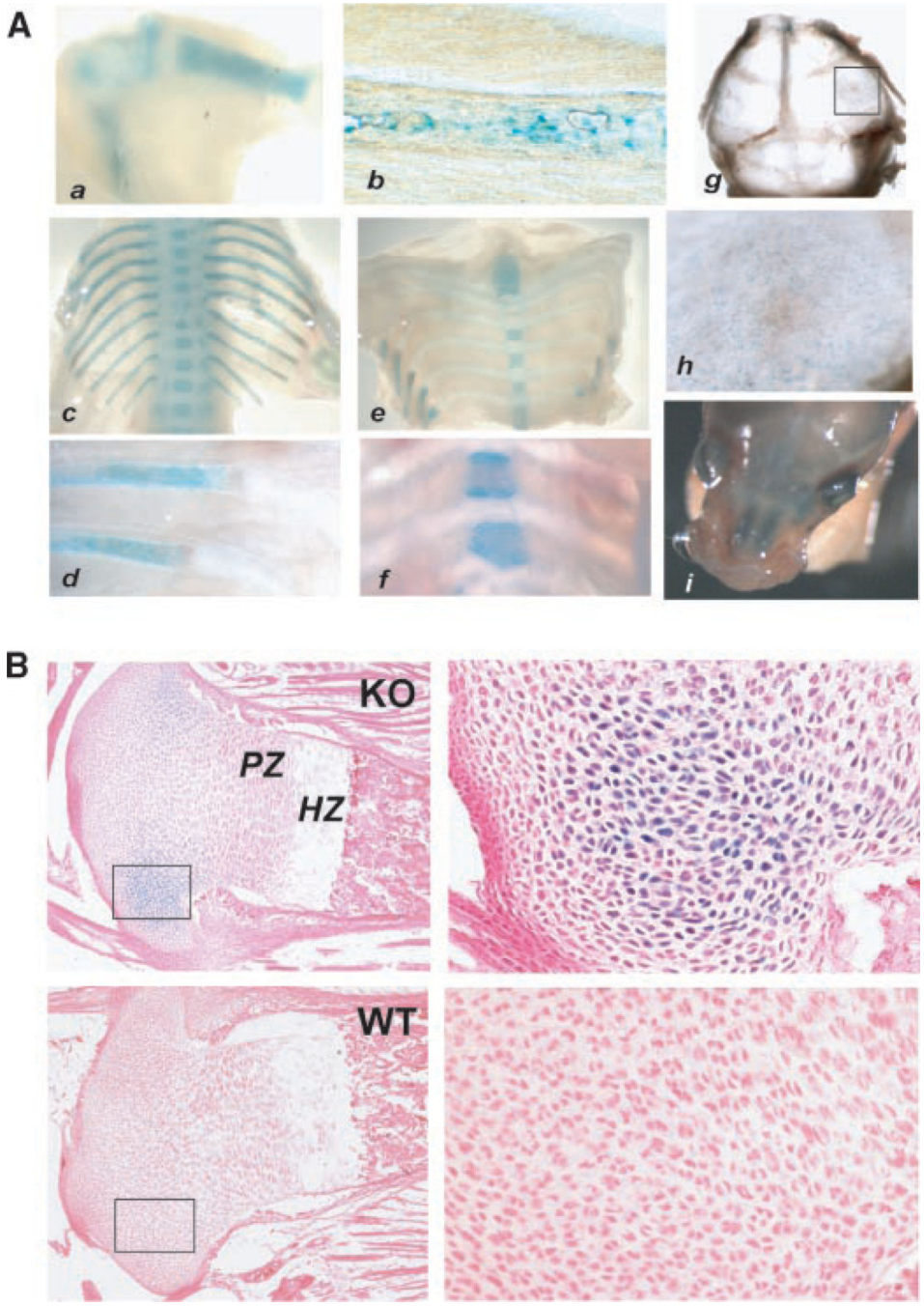

Fig. 3.

β-gal activity in skeletal structures of the sFRP1$^{-/-}$ mouse. A: sFRP1/β-gal activity in bone tissue. Parts a–f show β-gal staining of E17.5 and parts g–i, newborn. Skeletal tissues were dissected from embryo for photography at 1× (parts a,c,e) and 5× (parts b,d,f) using a Leica dissecting microscope. (a)Limbs; (b) femur; (c,d) vertebra and ribs; (e,f) sternebrae and cartilaginous portion of the ribs; Note staining in the vertebral bodies is strongest at the growth plates; (g) calvarium shows β-gal activity in bone tissue near the suture lines, boxed area shown a t 5× magnification (h); (i) ossifying nasal bones are observed to express sFRP1at birth and expression in the outer eye continues. B: sFRP1/β-gal activity (counterstained with eosin only) in cartilage at 2.5 × (left parts) and 10× (right parts) in KO and absence of staining in WT to demonstrate specificity.

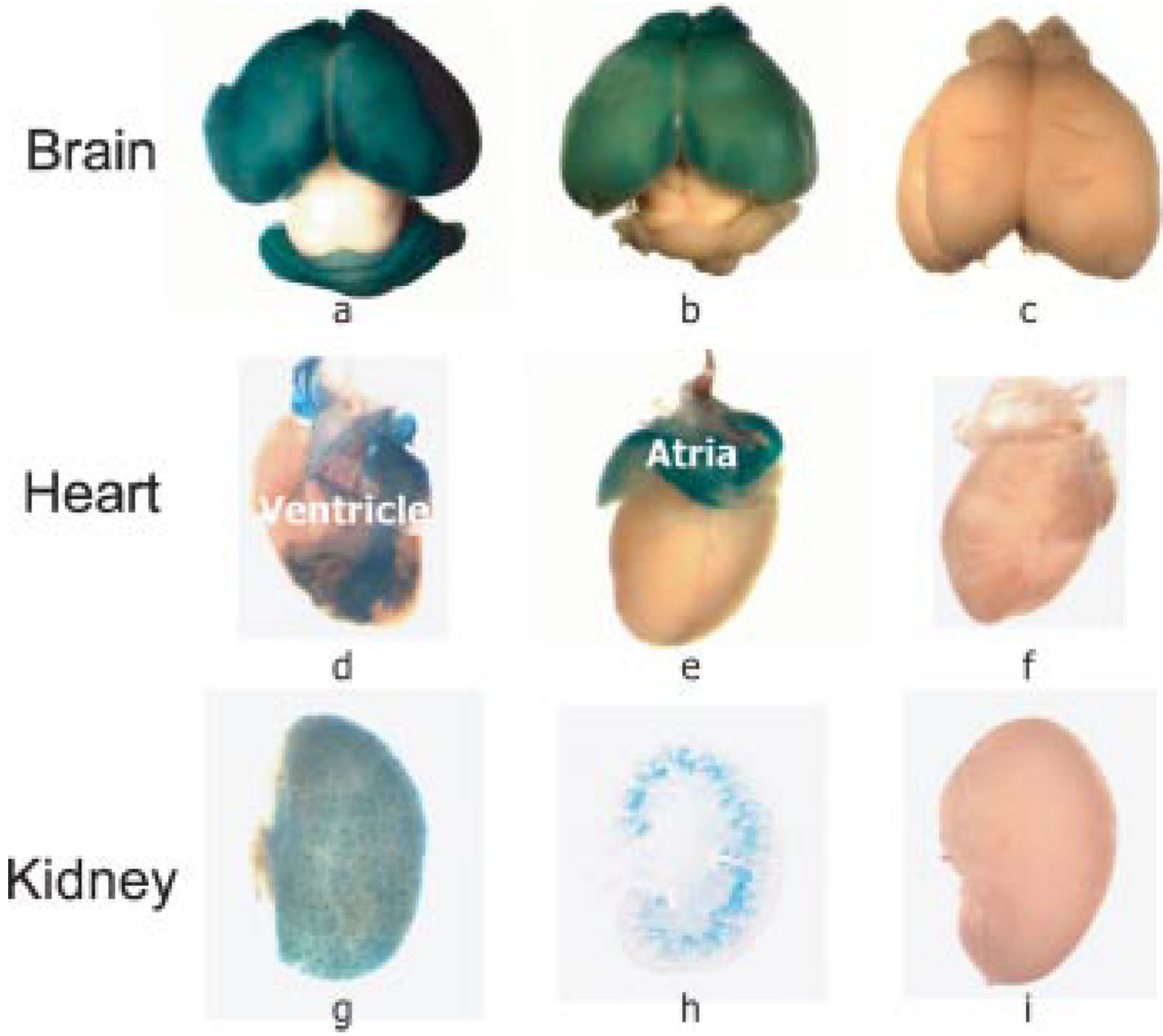

Fig. 4.

β-gal activity in post-natal soft tissues of the sFRP1$^{-/-}$ mouse. A: Three tissues with prominent LacZ staining were selected to demonstrate the persistence of high levels of sFRP1 transcriptional activity restricted to distinct areas of the tissue. Brain parts illustrate progression of change in sFRP1 expression from post-natal d7 (a) to d21 (b), at which time hind brain expression is not detected. Heart parts (d,e,f) on day 3 show posterior and anterior views of the heart (rotated 180°), to demonstrate β-gal activity in the aorta and left ventricle vessels. Kidney (g,h,i) shows β-gal activity on day 3 (g) that is associated with renal tubules in the cortex (h), identified in frozen sections (1×). WT controls in (c,f,i) show absence of β-gal activity. All WT (sFRP1$^{+/+}$) negative controls are stained under the same conditions (4 h, 37°C) as the sFRP1$^{-/-}$ knock-out mutant to demonstrate specificity of the β-gal enzymatic reaction. Five mice were used per genotype for each age. [Color figure can be viewed in the online issue, which is available at www.interscience.wiley.com.]

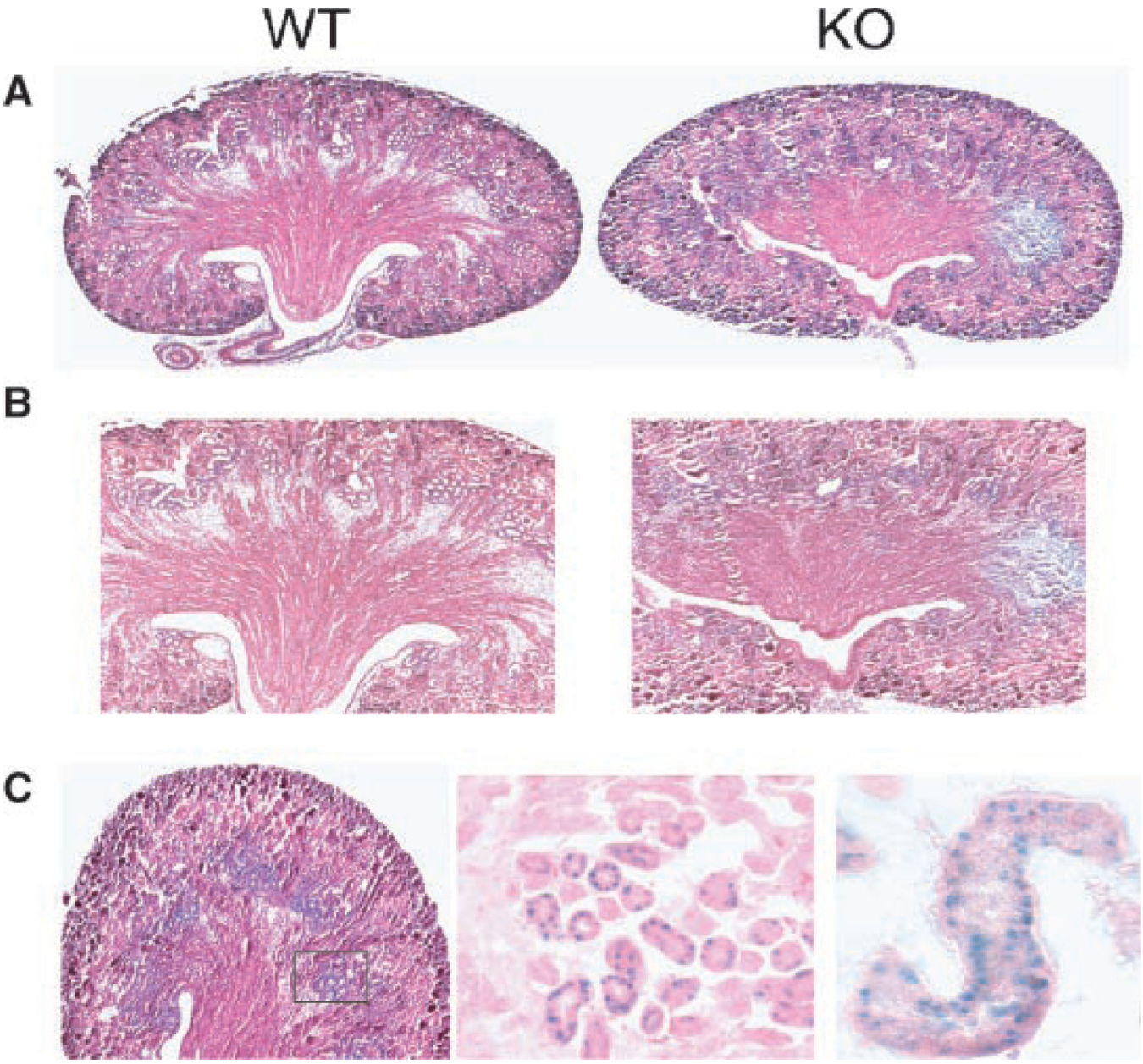

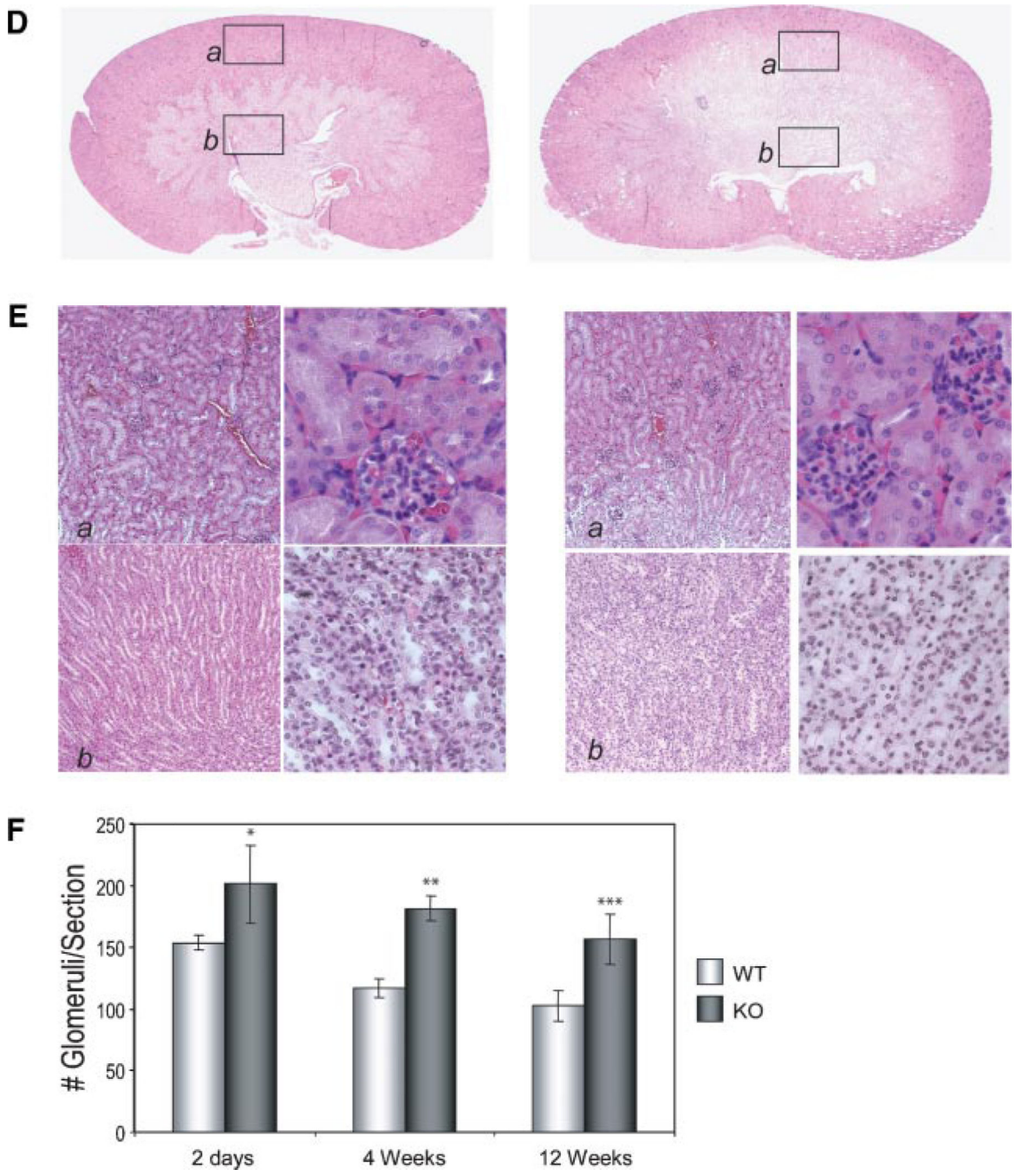

Fig. 5.

Kidney development and structure in the post-natal WT and KO mouse. A: Kidneys from newborn after β-gal staining of whole excised organ followed by fixation for paraffin section (2.5×) and higher magnifications (10×) of (B) cortex and (C) medulla. β-gal positive tubules and collecting duct are shown after β-gal staining with eosin only counterstain in middle part (10×) and right part (40×). Parts D and E show 4 weeks age kidney. Morphology (D) at 2.5× and (E) at 10× of the cortex (a) and (b) medulla left part, 10× and right part 40×. More glomeruli in the KO are found and along the corticomedullary junction. F: Quantitation of the number of glomeruli in n=4 unit areas per whole kidney section for n=5 slides representing different sections of the kidney. Glomeruli were counted at 10× magnification. The mean ± SEM for 20 total fields for n = 2 mice at each age is shown.

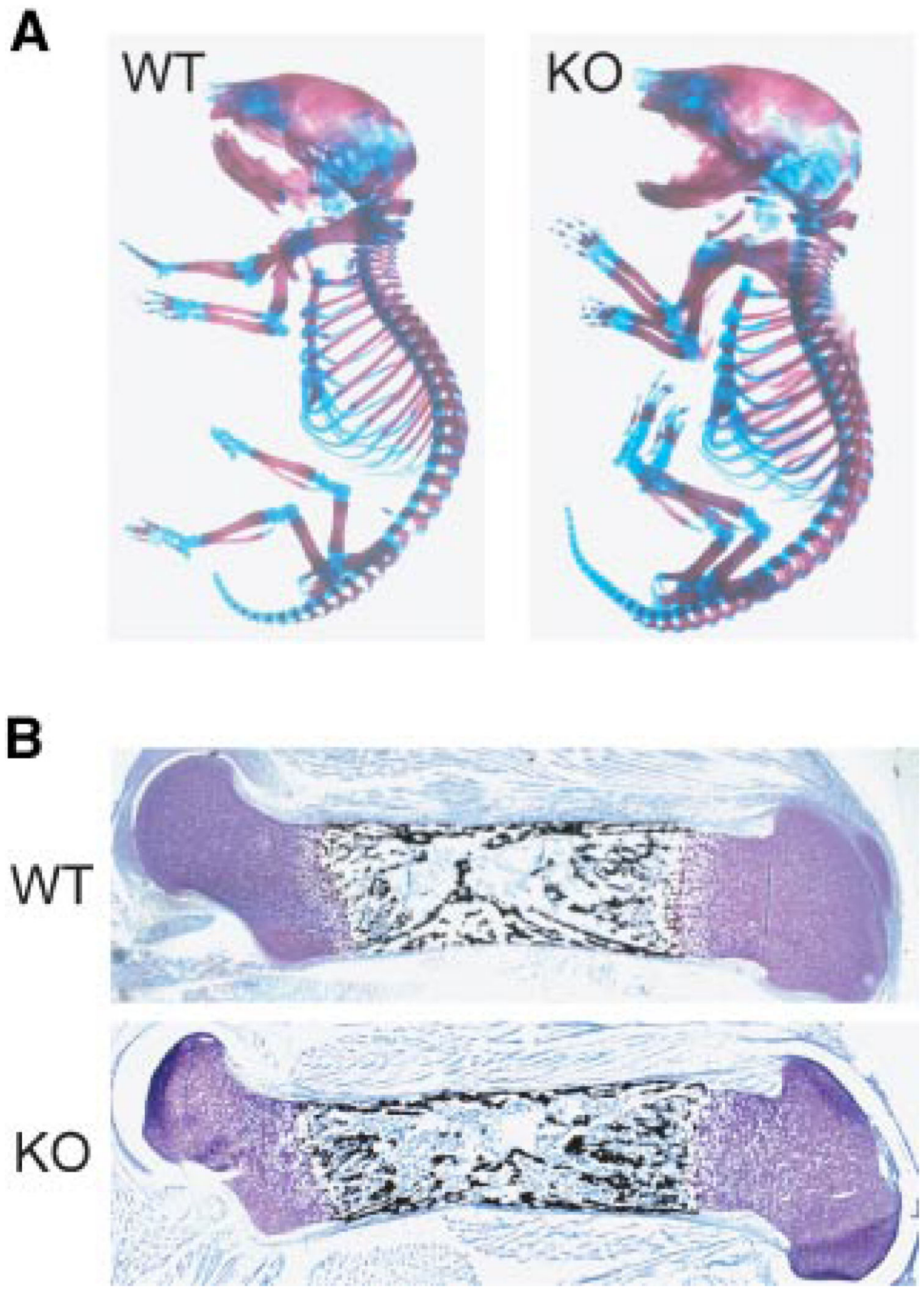

Fig. 6.

Normal development of the skeleton in the homozygous mouse lacking sFRP1. A: Alizarin Red and Alcian blue staining of skeletal preparations from the newborn WT and KO (sFRP1$^{-/-}$) mutant mouse. B: Histology of a mineralized femur with von Kossa silver stain and Toluidine blue counterstain, day 2 post-natal. [Color figure can be viewed in the online issue, which is available at www.interscience.wiley.com.]

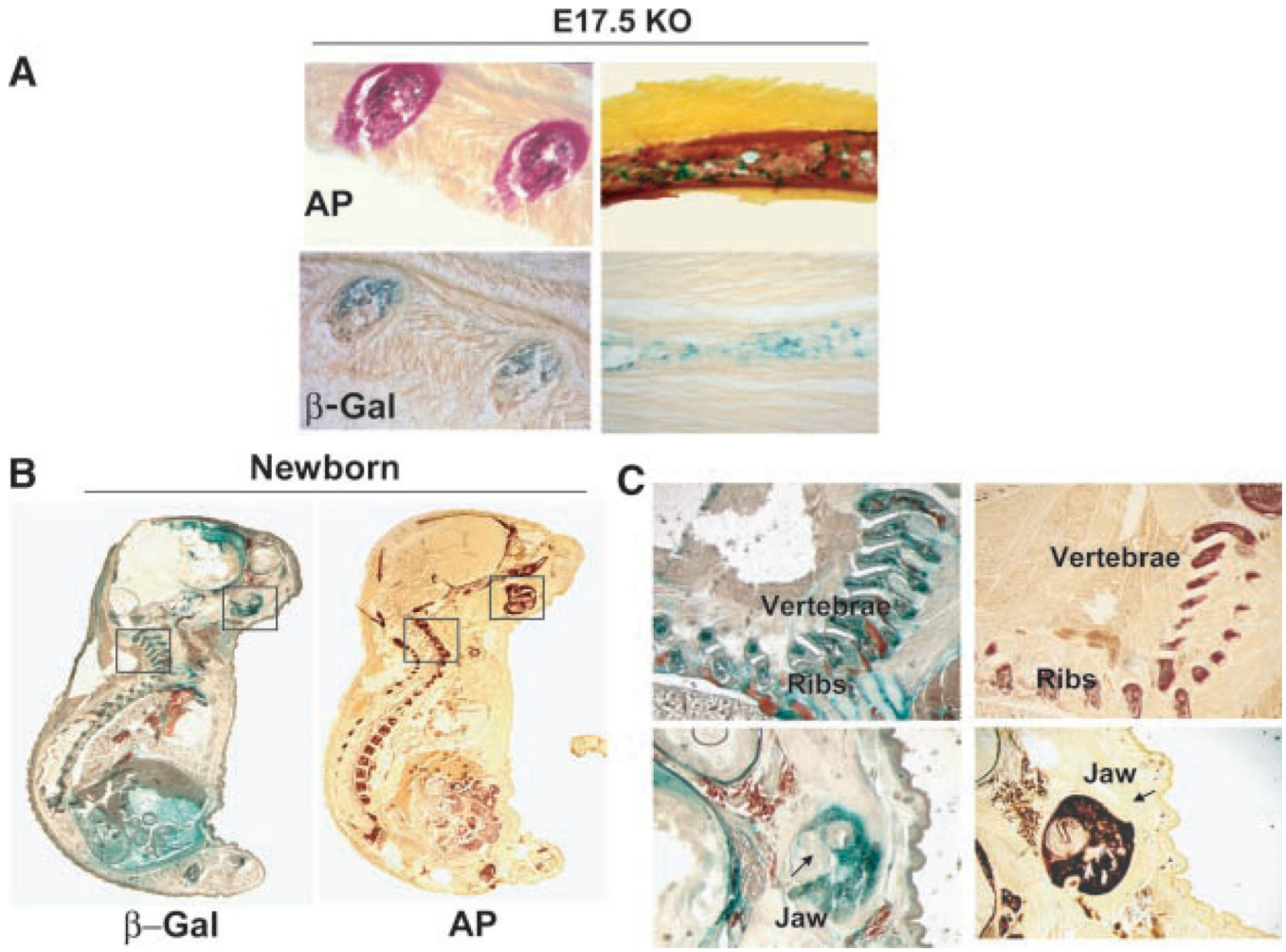

Fig. 7.

Expression of sFRP1 in calcified tissue of the axial skeleton. Frozen serial sections of the sFRP1$^{-/-}$ mouse were stained for alkaline phosphatase activity, a marker of skeletal mineralization and for β-gal activity. A: E17.5 sFRP1$^{-/-}$ shows cross sections of bony part of rib (left part), and longitudinal section in the right part (20×). Note the overlap of Alk Phos and β-gal activity. B: Newborn-whole embryo serial sections shows β-gal activity in vertebrae, ribs and craniofacial bones (left parts) and alkaline phosphatase (Alk Phos) activity (right parts). Enlargements of boxed areas are shown in (C) 5× magnification of mandible (jaw) and vertebrae.

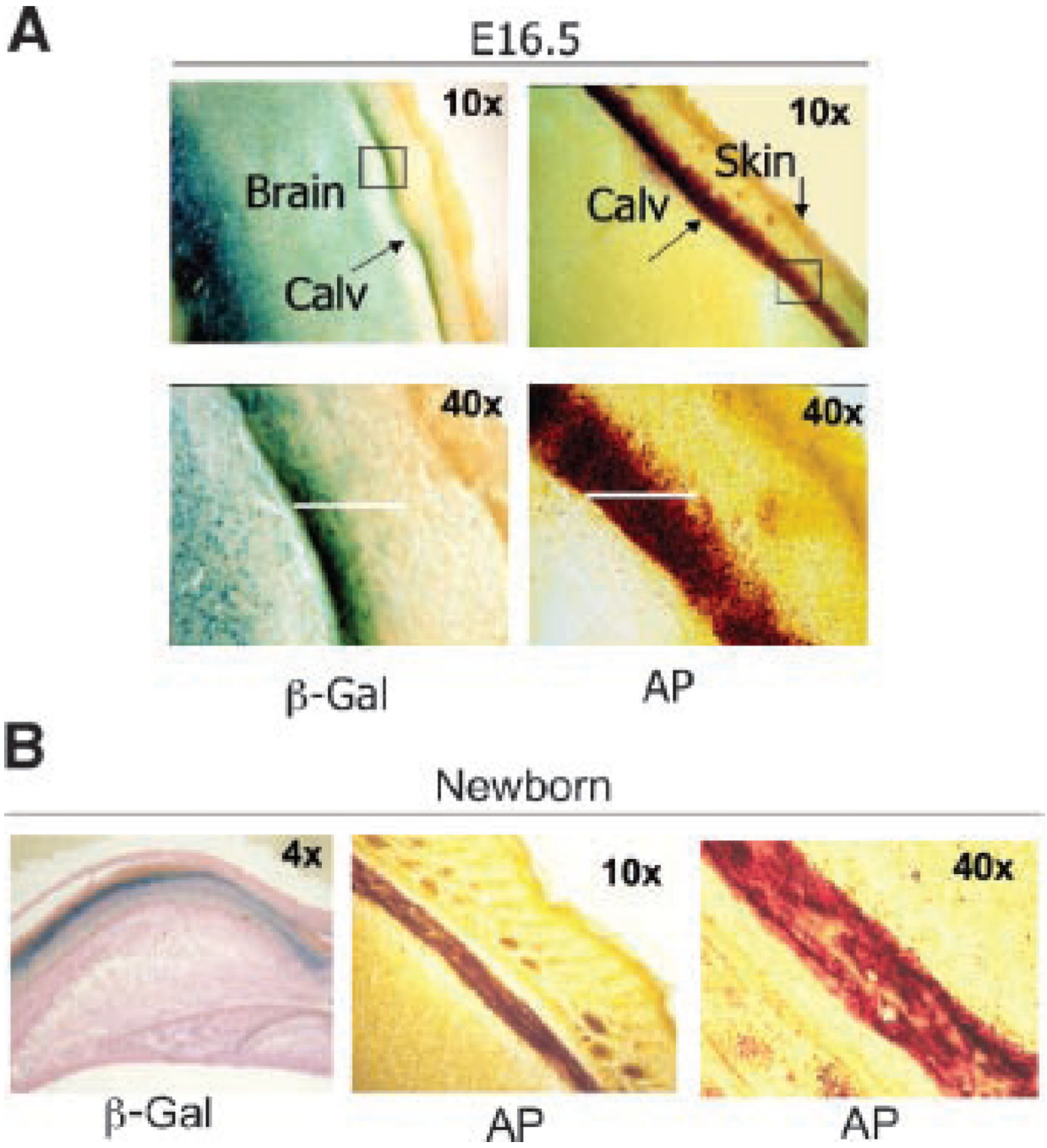

Fig. 8.

Coincidence of sFRP1 expression with the mineralization front of developing intramembranous bone tissue. Examination of calvarial bone. A: E 16.5 frozen sections from whole embryo. Left parts—β-gal; right parts—alkaline phosphatase (AP) activity of the sFRP1$^{-/-}$ mouse. Low magnification (10×) shows β-gal activity in the brain and in the bone tissue undergoing mineralization represented by alkaline phosphatase. The 40× magnification demonstrates the overlap of sFRP1 expression with the initial front of alkaline phosphatase staining and absence in the mature bone underlying the skin is demonstrated. B: sFRP1$^{-/-}$ newborn calvaria shows β-gal activity with eosin counterstain (left part) that overlaps alkaline phosphatase activity, shown at 10× (middle part) and 40× (right part).

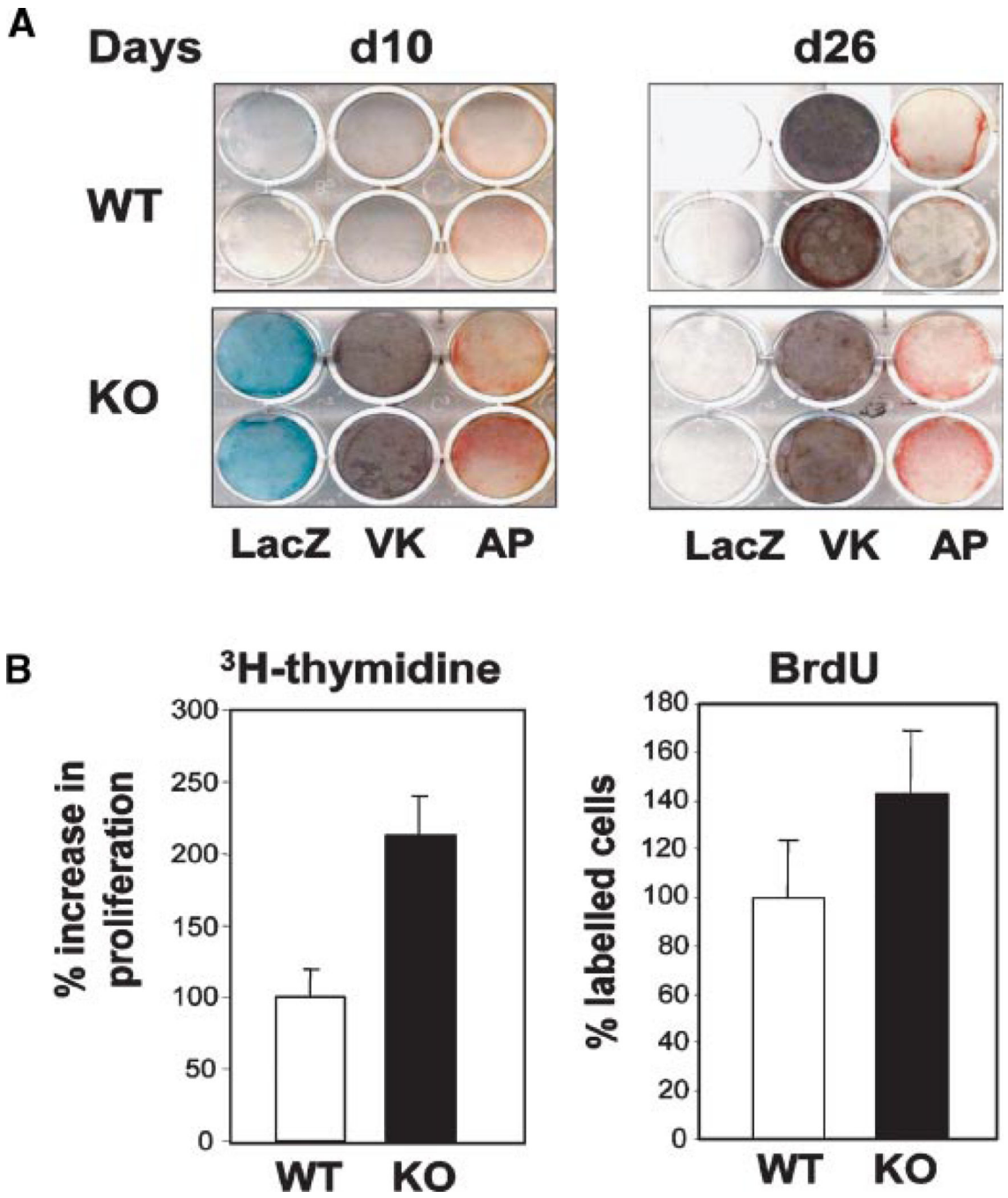

Fig. 9.

Ex vivo mouse calvarial osteoblasts from the sFRP-1$^{-/-}$ mouse exhibit increased AP activity. Calvarial osteoblasts were isolated from d2 pups (WT and KO) and cultured ex vivo. Calvaria (day3) dissected free of brain tissue used to isolate osteoblasts. The only positive β-gal activity is at the expanding bone between the parietal and occipital plates (data not shown). A: Representative β-gal, alkaline phosphatase and mineral (VK) stained cells d10 and d26 after plating. B: Cell proliferation measured biochemically by ^{3}H thymidine incorporation (left part, each bar represents n = 3 sample mean ± SD value) or by counting BrdU positive cells (right part, each part represents mean ± SD for n = 5 field). [Color figure can be viewed in the online issue, which is available at www.interscience.wiley.com.]

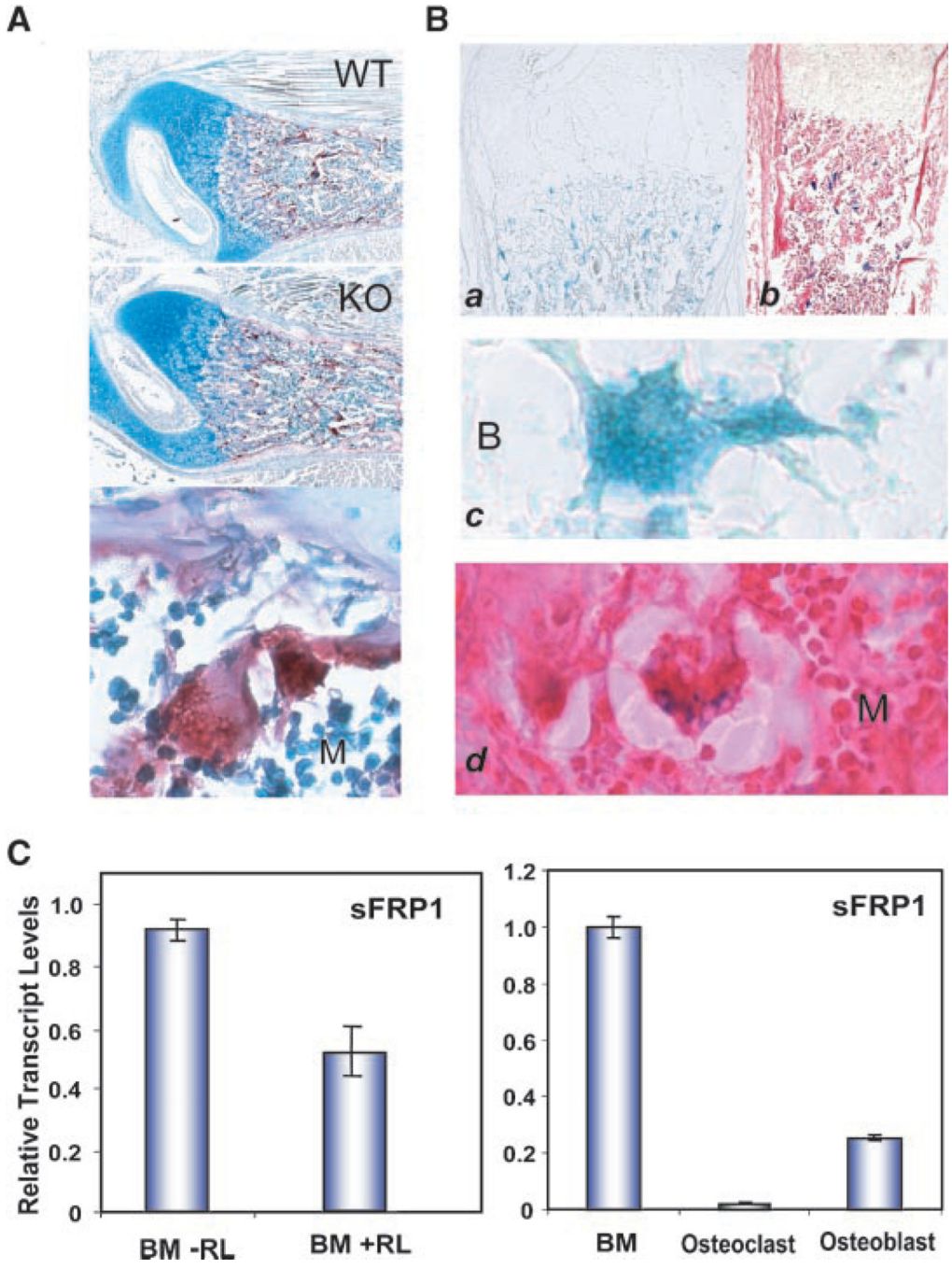

Fig. 10.

sFRP1 expression in osteoclasts. A: Tartrate resistant acid phosphatase staining of WT and KO mouse femur (paraffin 10×, day 2) with a 40× of osteoclast in lower part. B: β-gal activity, newborn femur 10× frozen section (a) and counterstained with eosin (b). Osteoclasts at 40× (c,d) from parts A and B, respectively. Bone surface (B) and marrow space (M) are shown. C: sFRP1 mRNA levels in osteoclasts. Left, normal bone marrow hematopoietic cells (from 8 weeks BalbC mice) and osteoclasts produced after 4 days of RANK ligand treatment, Right part—relative expression levels in undifferentiated bone marrow, osteoblasts and osteoclasts is compared. Q-PCR data obtained using Sybr-Green. sFRP1 is normalized to GAPDH and relative values compared in each sample (n=3 analysis).

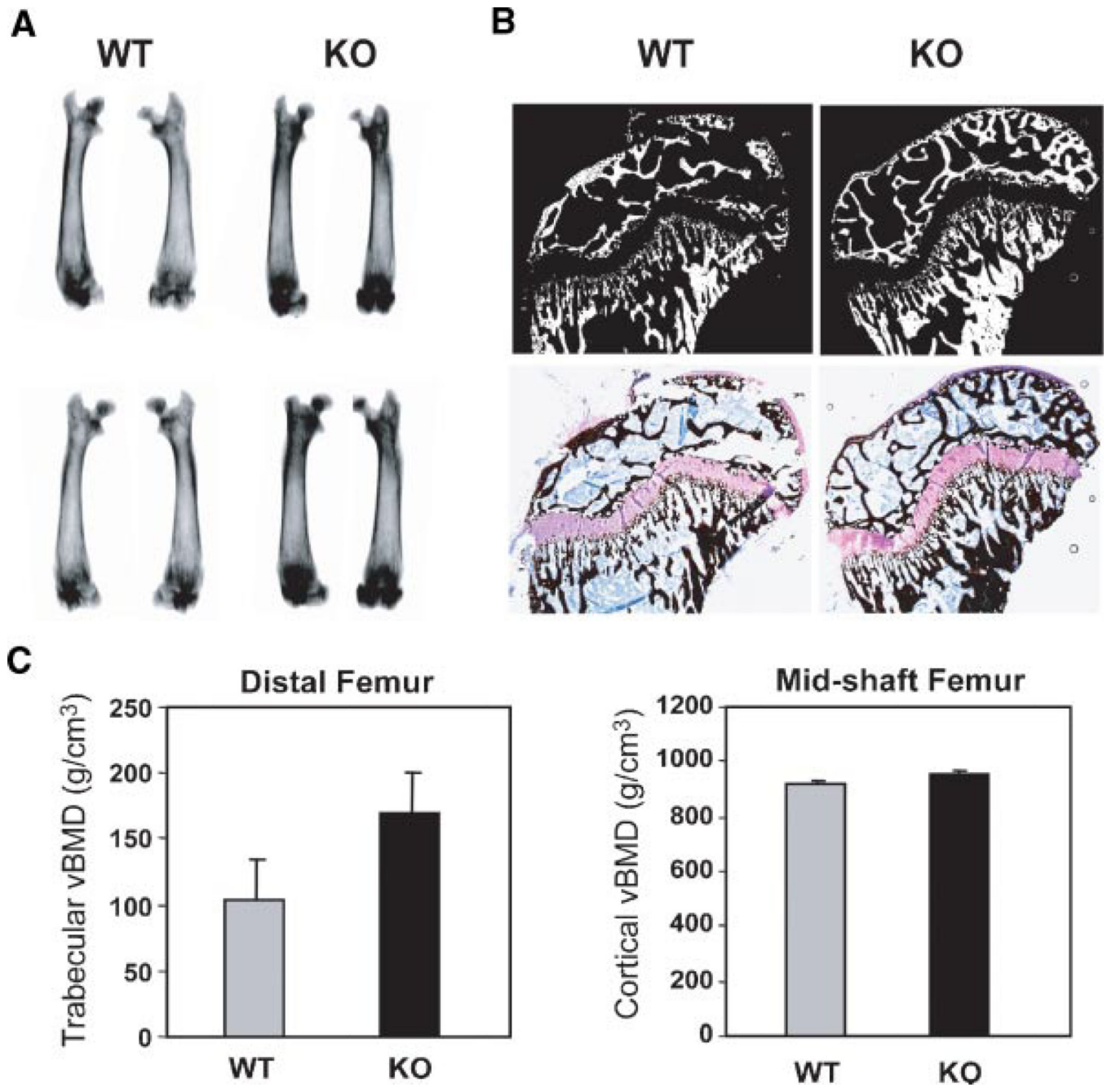

Fig. 11.

Trabecular bone density is increased in the 4 weeks age sFRP$^{-/-}$ mouse. A: Radiography of two examples of WT and KO femurs from different litters. B: Humerus bone showing mineralized areas of undecalcified sections embedded in plastic. Top part—reverse image of the Toluidine blue/von Kossa stained section shown in bottom part to emphasize mineralized tissue. C: DEXA analysis of volumetric bone mineral density of femurs (n = 3 mice/graph). [Color figure can be viewed in the online issue, which is available at www.interscience.wiley.com.]